

Conditional well-posedness and data-driven method for identifying the dynamic source in a coupled diffusion system from one single boundary measurement

Chunlong Sun^{*1,2}, Mengmeng Zhang^{†3}, and Zhidong Zhang^{‡4}

¹School of Mathematics, Nanjing University of Aeronautics and Astronautics, Nanjing 211106, Jiangsu, China

²Nanjing Center for Applied Mathematics, Nanjing 211135, Jiangsu, China

³School of Science, Hebei University of Technology, Tianjin 300401, China

⁴School of Mathematics (Zhuhai), Sun Yat-sen University, Zhuhai 519082, Guangdong, China

May 14, 2024

Abstract

This work considers the inverse dynamic source problem arising from the time-domain fluorescence diffuse optical tomography (FDOT). We recover the dynamic distributions of fluorophores in biological tissue by the one single boundary measurement in finite time domain. We build the uniqueness theorem of this inverse problem. After that, we introduce a weighted norm and establish the conditional stability of Lipschitz type for the inverse problem by this weighted norm. The numerical inversions are considered under the framework of the deep neural networks (DNNs). We establish the generalization error estimates rigorously derived from Lipschitz conditional stability of inverse problem. Finally, we propose the reconstruction algorithms and give several numerical examples illustrating the performance of the proposed inversion schemes.

Keywords: inverse dynamic source problem, uniqueness, conditional stability, deep neural networks, generalization error estimates, numerical inversion.

AMS Subject Classifications: 35R30, 65M32.

1 Introduction.

1.1 Background and mathematical model.

Fluorescence diffuse optical tomography (FDOT) is one type of diffuse optical tomography that uses fluorescence light from fluorophores in biological tissue, which is rapidly gaining acceptance as an important diagnostic and monitoring tool of symptoms in medical applications [2, 3]. The fluorescence contrast agents allow tracking non-invasively and quan-

^{*}sunchunlong@nuaa.edu.cn

[†]corresponding author: mmzhang@hebut.edu.cn

[‡]zhangzhidong@mail.sysu.edu.cn

titatively specific molecular events or provide some clinically important information *in vivo*. For FDOT, two processes are coupled, namely, *excitation* and *emission (fluorescence)*, which can be described by a coupled diffusion system as follows.

Let $\Omega \subset \mathbb{R}^d$ be the background medium with its boundary $\partial\Omega$. Let u_e, u_m be the photon density of excitation light and emission light, respectively. Furthermore, we consider the time-dependent fluorophores which means that the absorption coefficient μ_f depends on both x and t . Then we consider the following initial boundary value problems for u_e, u_m with $T < \infty$:

$$\begin{cases} (c^{-1}\partial_t + \mathcal{A}) u_e(x, t) = 0, & (x, t) \in \Omega \times (0, T), \\ u_e = 0, & (x, t) \in \Omega \times \{0\}, \\ \mathcal{B}u_e = g(x, t), & (x, t) \in \partial\Omega \times (0, T), \end{cases} \quad (1.1)$$

and

$$\begin{cases} (c^{-1}\partial_t + \mathcal{A}) u_m(x, t) = \mu_f(x, t)u_e(x, t) =: S[\mu_f, u_e], & (x, t) \in \Omega \times (0, T), \\ u_m = 0, & (x, t) \in \Omega \times \{0\}, \\ \mathcal{B}u_m = 0, & (x, t) \in \partial\Omega \times (0, T), \end{cases} \quad (1.2)$$

where μ_f denotes the dynamic distributions of fluorophores inside Ω . The elliptic operator \mathcal{A} and boundary condition \mathcal{B} are defined as

$$\begin{cases} \mathcal{A}\psi = -\nabla \cdot (\kappa(x)\nabla\psi) + \mu_a(x)\psi, & \psi \in H^2(\Omega), \\ \mathcal{B}\psi = \left(\frac{\partial\psi}{\partial\mathbf{n}} + \beta\psi \right) \Big|_{\partial\Omega}, \end{cases} \quad (1.3)$$

where $\beta > 0$ is the Robin coefficient; $\kappa(x)$ is the diffusion coefficient; μ_a is the absorption coefficient of background medium. The time-domain FDOT is a method to achieve imaging of μ_f from the boundary data given by

$$\varphi(x, t) = \frac{\partial u_m}{\partial\mathbf{n}} \Big|_{\Gamma \times (0, T)}, \quad (1.4)$$

where Γ is a nonempty open subset of boundary $\partial\Omega$.

In the aspect of theoretical analysis, the uniqueness of recovering $\mu_f(x, t)$ requires the whole information of u_m on $\Omega \times (0, T)$, but it is impractical in applications. However, although the boundary measurement as in (1.4) is practical, it is not sufficient to uniquely reconstruct $\mu_f(x, t)$ and its uniqueness is almost open. Actually, even for recovering the stationary fluorophores (i.e., $\mu_f(x, t) \equiv \mu_f(x)$) from (1.4), the literature on the uniqueness is relatively rare. An identifiability result of absorption coefficient $\mu_f(x)$ is established in [23], but it requires strong prior assumptions on $\mu_f(x)$. The authors prove that for $\Omega = \mathbb{R}_+^3$, $x = (\tilde{x}, x_3) \in \mathbb{R}^2 \times \mathbb{R}_+^1$, by supposing $\mu_f(x)$ has the variable separable form $\mu_f(x) = p(\tilde{x})q(x_3)$ with known vertical information $q(x_3)$, the horizontal information $p(\tilde{x})$ can be uniquely determined from the boundary measurement (1.4) with $\Gamma = \partial\Omega$. Assuming that the support of $\mu_f(x)$ is at a point, called a point target, the minimal number of observation detectors to determine the point target location as well as its local stability are investigated in [19].

In this work, we study the inverse problem of recovering the dynamic source $\mu_f(x, t)$ from boundary data (1.4). Suppose that $S[\mu_f, u_e](x, t; x_s)$ in (1.2) possesses the following semi-discrete formulation:

$$S[\mu_f, u_e] = \sum_{k=1}^K p_k(x) \chi_{t \in [t_{k-1}, t_k)}, \quad (1.5)$$

where χ is the indicator function, the time mesh $\{t_k\}_{k=0}^K$ is given and the spatial components $\{p_k(x)\}_{k=1}^K$ are undetermined. For the unknown $\{p_k(x)\}_{k=1}^K$, we consider to recover them in $L^2(\Omega)$. Since the excitation u_e is known, after solving $\{p_k(x)\}_{k=1}^K$, the values of $\{\mu_f(\cdot, t_k)\}_{k=0}^{K-1}$ can be recovered as $\mu_f(\cdot, t_k) = p_{k+1}(\cdot)/u_e(\cdot, t_k)$, $k = 0 \cdots, K-1$. We conclude the inverse problem of time-domain FDOT as follows:

$$\text{recovering } \{p_k(x)\}_{k=1}^K \text{ in (1.5) from the one single boundary measurement (1.4).} \quad (1.6)$$

1.2 Literature and outline.

The inverse problem (1.6) has not been rigorously investigated as far as we know. With the Laplace transform and the knowledge of complex analysis, [22, 41] established the uniqueness theorem of inverse problem (1.6) but required $T = \infty$. In this work, we will consider the uniqueness of recovering $\{p_k(x)\}_{k=1}^K$ by the boundary measurement in finite time domain ($T < \infty$). Furthermore, we will define a weighted norm and establish the conditional stability of Lipschitz type for the inverse problem (1.6) by the defined weighted norm. The defined weighted norm is a little bit weaker than the standard L^2 norm. Hence the obtained stability result will be the conditional stability for our inverse problem in $L^2(\Omega)$ by some weighted norm.

Numerically, for the forward problem of FDOT, F.Martelli et al [30] and H.B.Jiang [16] summarized the principles and applications of light propagation through biological tissue and other diffusive media, and gave the theory, solutions and software codes, respectively. For the inverse problem of FDOT, the necessary regularization techniques such as Tikhonov regularization, sparse regularization methods and hybrid regularization methods have been introduced to overcome the ill-posedness of the inverse problems [7, 10, 24]. To solve the inverse problem, the gradient-type iteration such as Landweber iteration [14] and the Newton-type iteration such as Levenberg–Marquardt method [5, 13, 21, 29], the iteratively regularized Gauss-Newton method [18, 20] are common iterative methods. [2, 3] presented a review of methods for the forward and inverse problems in optical tomography. However, most existing works focus on recovering the stationary $\mu_f(x)$, the inversion of dynamic $\mu_f(x, t)$ in (1.6) is still a challenging problem.

Recently, deep learning methods for solving PDEs have been realized as an effective approach, especially in high dimensional PDEs. Such methods have the advantage of breaking the curse of dimensionality. The basic idea is to use neural networks (nonlinear functions) to approximate the unknown solutions of PDEs by learning the networks parameters. For the forward problems, there exists many numerical works with deep neural networks involving the deep Ritz method (DRM) [11], the deep Galerkin method (DGM) [38], the DeepXDE method [26], deep operator network method (DeepONet) [25], physical information neural networks (PINNs) [32], the weak adversary neural network (WAN) [4, 42] and so on. Theoretically, there are some rigorous analysis works investigating the convergence and error estimates for the solution of PDEs via neural networks, but the result are still far from complete. For example, the convergence rate of DRM with two layer networks and deep networks were studied in [9, 15, 27, 28]; the convergence of PINNs was given in [17, 31, 8, 35, 36]. For the inverse problems, the PINNs frameworks can be employed to solve the so-called data assimilation or unique continuation problems, and rigorous estimates on the generalization error of PINNs were established in [31]. Bao et al [42] developed the WAN to solve electrical impedance tomography (EIT) problem. In [43], the authors studied a classical linear inverse

source problem using the final time data under the frameworks of neural networks, where a rigorous generalization error estimate is proposed with a novel loss function including the Sobolev norm of some residuals. For more specific inverse problems applied in engineering and science, we refer to [6, 33, 37].

In this work, we consider the reconstruction of the dynamic source of the inverse problem (1.6) parameterized by deep neural networks (DNNs). For the emission process, a new loss function is proposed with regularization terms depending on the derivatives of the residuals for PDEs and measurement data. We establish generalization error estimates rigorously derived from Lipschitz conditional stability of inverse problems. Furthermore, we propose the reconstruction scheme and make some numerical implementations to demonstrate the validity of the reconstruction algorithm.

The rest of this article is organized as follows. In Section 2, we collect several preliminary works. We prove the uniqueness theorem and the condition stability in Section 3, which are stated in Theorems 1 and 2. The numerical inversions will be considered in Section 4. The authors introduce the loss functions and build generalization error estimates in Theorem 3. Then the reconstruction algorithms and some numerical experiments are provided in Section 5, which can verify the theories.

2 Preliminaries.

2.1 Eigensystem of operator \mathcal{A} .

For the operator \mathcal{A} on $H^2(\Omega)$ with Robin boundary condition, we denote the eigensystem by $\{\lambda_n, \varphi_n(x)\}_{n=1}^\infty$. Then the following properties will be valid:

- $0 < \lambda_1 \leq \lambda_2 \leq \dots$ and $\lambda_n \rightarrow \infty$ as $n \rightarrow \infty$;
- $\{\varphi_n\}_{n=1}^\infty \subset H^2(\Omega)$ is an orthonormal basis of $L^2(\Omega)$.

Furthermore, if φ_n is an eigenfunction of \mathcal{A} corresponding to λ_n , so is $\overline{\varphi_n}$, where $\overline{\varphi_n}$ is the complex conjugate of φ_n . Hence we have that the set $\{\varphi_n(x)\}_{n=1}^\infty$ coincides with $\{\overline{\varphi_n(x)}\}_{n=1}^\infty$. The trace theorem yields that $\{\frac{\partial \varphi_n}{\partial \mathbf{H}}|_{\partial\Omega}\}_{n=1}^\infty \subset H^{1/2}(\partial\Omega)$. Also, we denote $\langle \cdot, \cdot \rangle_{\kappa, \partial\Omega}$ as the weighted inner product in $L^2(\partial\Omega)$.

The next lemmas concern the vanishing property and the density of $\frac{\partial \varphi_n}{\partial \mathbf{H}}$ on $\partial\Omega$.

Lemma 2.1. *If Γ is a nonempty open subset of $\partial\Omega$, then for each $n \in \mathbb{N}^+$, $\frac{\partial \varphi_n}{\partial \mathbf{H}}$ can not vanish on Γ .*

Proof. See [22, Lemma 2.1]. □

Lemma 2.2. *The set $\text{Span}\{\frac{\partial \varphi_n}{\partial \mathbf{H}}|_{\partial\Omega}\}_{n=1}^\infty$ is dense in $L^2(\partial\Omega)$.*

Proof. Not hard to see that $H^{3/2}(\partial\Omega)$ is dense in $L^2(\partial\Omega)$ under the norm $\|\cdot\|_{L^2(\partial\Omega)}$. So it is sufficient to show $\tilde{\psi} \in H^{3/2}(\partial\Omega)$ vanishes almost everywhere on $\partial\Omega$ if $\langle \tilde{\psi}, \frac{\partial \varphi_n}{\partial \mathbf{H}} \rangle_{\kappa, \partial\Omega} = 0$ for $n \in \mathbb{N}^+$.

We set ψ be the weak solution of the system below:

$$\begin{cases} \mathcal{A}\psi(x) = 0, & x \in \Omega, \\ \mathcal{B}\psi = \tilde{\psi}, & x \in \partial\Omega. \end{cases}$$

We have $\psi \in H^2(\Omega)$ from the regularity $\tilde{\psi} \in H^{3/2}(\partial\Omega)$, sequentially the Green's identity can be used. For $n \in \mathbb{N}^+$, we have

$$\begin{aligned} \langle \mathcal{A}\psi, \varphi_n \rangle_\Omega - \langle \psi, \mathcal{A}\varphi_n \rangle_\Omega &= \langle \psi, \frac{\partial \varphi_n}{\partial \bar{\mathbf{H}}} \rangle_{\kappa, \partial\Omega} - \langle \frac{\partial \psi}{\partial \bar{\mathbf{H}}}, \varphi_n \rangle_{\kappa, \partial\Omega} \\ &= \langle \psi + \beta \frac{\partial \psi}{\partial \bar{\mathbf{H}}}, \frac{\partial \varphi_n}{\partial \bar{\mathbf{H}}} \rangle_{\kappa, \partial\Omega} \\ &= \langle \tilde{\psi}, \frac{\partial \varphi_n}{\partial \bar{\mathbf{H}}} \rangle_{\kappa, \partial\Omega}. \end{aligned}$$

From $\mathcal{A}\psi = 0$ on Ω and the fact $\langle \tilde{\psi}, \frac{\partial \varphi_n}{\partial \bar{\mathbf{H}}} \rangle_{\kappa, \partial\Omega} = 0$, we have

$$\langle \psi, \mathcal{A}\varphi_n \rangle_\Omega = \lambda_n \langle \psi, \varphi_n \rangle_\Omega = 0.$$

So we have proved that for each $n \in \mathbb{N}^+$, $\langle \psi, \varphi_n \rangle_\Omega = 0$. Recalling the completeness of $\{\varphi_n\}_{n=1}^\infty$ in $L^2(\Omega)$, it holds that $\|\psi\|_{L^2(\Omega)} = 0$. From the definition of weak derivative and Sobolev space, we have $\|\psi\|_{H^2(\Omega)} = 0$. By the continuity of the trace operator, it gives that

$$\|\psi\|_{L^2(\partial\Omega)} \leq C\|\psi\|_{H^2(\Omega)} = 0, \quad \left\| \frac{\partial \psi}{\partial \bar{\mathbf{H}}} \right\|_{L^2(\partial\Omega)} \leq C\|\psi\|_{H^2(\Omega)} = 0.$$

This means that $\tilde{\psi} = 0$ almost everywhere on $\partial\Omega$ and the proof is complete. \square

2.2 The auxiliary functions $\{\xi_l\}_{l=1}^\infty$ and the coefficients $\{c_{z,n}\}$.

From the above lemma, we are allowed to construct the orthonormal basis $\{\tilde{\xi}_l\}_{l=1}^\infty$ in $L^2(\kappa, \partial\Omega)$. Firstly we set $\tilde{\xi}_1 = \frac{\partial \varphi_1}{\partial \bar{\mathbf{H}}} |_{\partial\Omega} / \|\frac{\partial \varphi_1}{\partial \bar{\mathbf{H}}}\|_{L^2(\kappa, \partial\Omega)}$, and assume that the orthonormal set $\{\tilde{\xi}_j\}_{j=1}^{l-1}$ has been built for $l = 2, 3, \dots$. Then we set $n_l \in \mathbb{N}^+$ be the smallest number such that $\frac{\partial \varphi_{n_l}}{\partial \bar{\mathbf{H}}} |_{\partial\Omega} \notin \text{Span}\{\tilde{\xi}_j\}_{j=1}^{l-1}$, and pick $\tilde{\xi}_l \in \text{Span}\{\frac{\partial \varphi_{n_l}}{\partial \bar{\mathbf{H}}} |_{\partial\Omega}, \tilde{\xi}_1, \dots, \tilde{\xi}_{l-1}\}$ satisfying

$$\langle \tilde{\xi}_l, \tilde{\xi}_j \rangle_{\kappa, \partial\Omega} = 0 \text{ for } j = 1, \dots, l-1, \text{ and } \|\tilde{\xi}_l\|_{L^2(\kappa, \partial\Omega)} = 1.$$

The density of $\text{Span}\{\frac{\partial \varphi_n}{\partial \bar{\mathbf{H}}} |_{\partial\Omega}\}_{n=1}^\infty$ in $L^2(\kappa, \partial\Omega)$ yields that $\{\tilde{\xi}_l\}_{l=1}^\infty$ is an orthonormal basis in $L^2(\kappa, \partial\Omega)$. Also, we have $\tilde{\xi}_l \in H^{1/2}(\partial\Omega)$ for each $l \in \mathbb{N}^+$.

Next, for $l \in \mathbb{N}^+$, we define $\xi_l \in H^1(\Omega)$ be the weak solution of the system:

$$\begin{cases} \mathcal{A}\xi_l(x) = 0, & x \in \Omega, \\ \mathcal{B}\xi_l = \tilde{\xi}_l, & x \in \partial\Omega. \end{cases} \quad (2.1)$$

Fixing $z \in \partial\Omega$, we define the series $\psi_z^N \in H^1(\Omega)$ as

$$\psi_z^N(x) = \sum_{l=1}^N \tilde{\xi}_l(z) \overline{\tilde{\xi}_l(x)}, \quad x \in \Omega. \quad (2.2)$$

The finite summation ψ_z^N is constructed following the role of Dirac delta function, which reflects the information of the targeted function on a specific point via integration. With the following lemma, we can give the coefficients $\{c_{z,n}\}$.

Lemma 2.3. *For each $z \in \partial\Omega$ and $n \in \mathbb{N}^+$, $\lim_{N \rightarrow \infty} \langle \psi_z^N, \overline{\varphi_n} \rangle_\Omega$ exists and we denote the limit by $c_{z,n}$.*

Proof. From Green's identities we have

$$\begin{aligned} \langle \psi_z^N, \overline{\varphi_n} \rangle_\Omega &= \lambda_n^{-1} \langle \psi_z^N, \mathcal{A}\overline{\varphi_n} \rangle_\Omega \\ &= \lambda_n^{-1} \left(\langle \mathcal{A}\psi_z^N, \overline{\varphi_n} \rangle_\Omega - \langle \psi_z^N, \frac{\partial \overline{\varphi_n}}{\partial \mathbf{n}} \rangle_{\kappa, \partial\Omega} + \langle \frac{\partial \psi_z^N}{\partial \mathbf{n}}, \overline{\varphi_n} \rangle_{\kappa, \partial\Omega} \right) \\ &= -\lambda_n^{-1} \langle \beta \frac{\partial \psi_z^N}{\partial \mathbf{n}} + \psi_z^N, \frac{\partial \overline{\varphi_n}}{\partial \mathbf{n}} \rangle_{\kappa, \partial\Omega} \\ &= -\lambda_n^{-1} \sum_{l=1}^N \tilde{\xi}_l(z) \langle \frac{\partial \varphi_n}{\partial \mathbf{n}}, \tilde{\xi}_l \rangle_{\kappa, \partial\Omega} =: c_{z,n}^N, \end{aligned}$$

where the system (2.1) and the boundary condition of φ_n are used. From the definition of $\{\tilde{\xi}_l\}_{l=1}^\infty$, we have $\langle \frac{\partial \varphi_n}{\partial \mathbf{n}}, \tilde{\xi}_l \rangle_{\kappa, \partial\Omega} = 0$ for large l . Hence the value of $c_{z,n}^N$ will not change if N is sufficiently large. This gives that $\lim_{N \rightarrow \infty} \langle \psi_z^N, \overline{\varphi_n} \rangle_\Omega$ exists and the proof is complete. \square

Then we consider the following system and denote the solutions by $\{u_z^N\}$:

$$\begin{cases} (c^{-1}\partial_t + \mathcal{A})u_z^N(x, t) = 0, & (x, t) \in \Omega \times (0, \infty), \\ \mathcal{B}u_z^N(x, t) = 0, & (x, t) \in \partial\Omega \times (0, \infty), \\ u_z^N(x, 0) = -\psi_z^N, & x \in \Omega. \end{cases} \quad (2.3)$$

With the coefficients $\{c_{z,n}\}$ and defining $p_{k,n} := \langle p_k(\cdot), \varphi_n(\cdot) \rangle_\Omega$, we give the next assumptions, which will be used in the proof of uniqueness and conditional stability.

Assumption 2.4.

- (a) *For $k \in \{1, \dots, K\}$ and a.e. $z \in \partial\Omega$, there exists $C > 0$ which is independent of N such that $\sum_{n=1}^\infty |c_{z,n}^N p_{k,n}| < C < \infty$ for each $N \in \mathbb{N}^+$.*
- (b) *For a.e. $z \in \partial\Omega$, it holds that $\sum_{k=1}^K \sum_{n=1}^\infty |c_{z,n} p_{k,n}| < \infty$.*
- (c) *For a.e. $t \in [0, \infty)$, the spatial components $\{p_k(x)\}_{k=1}^K$ are smooth enough such that the series $\sum_{l=1}^\infty \tilde{\xi}_l(x) \langle \frac{\partial u}{\partial \mathbf{n}}(\cdot, t), \tilde{\xi}_l(\cdot) \rangle_{\kappa, \partial\Omega}$ converges to $\frac{\partial u}{\partial \mathbf{n}}(x, t)$ pointwisely for a.e. $x \in \partial\Omega$.*

2.3 General settings of deep neural networks.

For better readability, we introduce some general settings of deep neural networks. Numerically, we parameterize the excitation u_e , emission u_m as well as the unknown μ_f by deep neural networks, given by u_{e,θ_e} , u_{m,θ_m} and μ_{f,θ_f} , respectively. Here θ_e , θ_m and θ_f are the corresponding network parameters. The loss functions to determine the optimal network parameters and related generalization error estimates will be investigated in Section 4, whereas we give the network architecture and the quadrature rule in computing the loss functions.

Network architecture. Noting that u_{e,θ_e} , u_{m,θ_m} and μ_{f,θ_f} are several separate networks with arguments (x, t) . Thus, we use ξ to denote collectively the network parameters which are bounded for a parametric function $s_\xi(z)$ such that a general scheme can be applied for either $u_{e,\theta_e}(x, t)$, $u_{m,\theta_m}(x, t)$ or $\mu_{f,\theta_f}(x, t)$ (with $z = (x, t)$, $\xi = \theta$).

For a positive integer $K \in \mathbb{N}$, a K -layer feed-forward neural network of $s_\xi(z)$ for $z \in \mathbb{R}^{d_0}$ is a function defined by

$$s_\xi(z) := W_K l_{K-1} \circ \cdots \circ l_1(z) + b_K, \quad (2.4)$$

where the k -th layer $l_k : \mathbb{R}^{d_{k-1}} \rightarrow \mathbb{R}^{d_k}$ is given by $l_k(z) = \sigma(W_k z + b_k)$ with weights $W_k \in \mathbb{R}^{d_k \times d_{k-1}}$ and biases $b_k \in \mathbb{R}^{d_k}$ for $k = 2, \dots, K$, and $\sigma(\cdot)$ is the activation function. The network parameters of all layers are collectively denoted by

$$\xi := (W_K, b_K, W_{K-1}, b_{K-1}, \dots, W_1, b_1).$$

Quadrature rules [31]. We also need to state the quadrature rules applied for approximately computing the integrals in the loss function. Consider a mapping $h : \mathbb{D} \subset \mathbb{R}^{\bar{d}} \mapsto \mathbb{Y} \subset \mathbb{R}^m$. To approximate the integral

$$\bar{h} := \int_{\mathbb{D}} h(y) dy$$

numerically by a quadrature rule with dy being the \bar{d} -dimensional Lebesgue measure, we need the quadrature points $y_i \in \mathbb{D}$ for $i = 1, 2, \dots, N$ as well as the weights $w_i \in \mathbb{R}_+$. Then a quadrature formula is defined by

$$\bar{h}_N := \sum_{i=1}^N w_i h(y_i).$$

We further assume that the quadrature error is

$$|\bar{h} - \bar{h}_N| \leq C_q (\|h\|_{\mathbb{Y}}, \bar{d}) N^{-\alpha} \quad (2.5)$$

for some $\alpha > 0$, which is well-known for several classical quadrature formulas.

3 The uniqueness and conditional stability.

3.1 Representation of the forward operator.

To investigate the inverse problem, we firstly give the representation formula of the forward operator, which maps the unknown source to the boundary flux data. With a small $\epsilon > 0$ we give the following equation

$$\begin{cases} (c^{-1} \partial_t + \mathcal{A})u(x, t) = p(x), & (x, t) \in \Omega \times (0, \epsilon), \\ u(x, t) = 0, & (x, t) \in \partial\Omega \times (0, \epsilon) \cup \Omega \times \{0\}, \end{cases} \quad (3.1)$$

and prove the next lemma for equation (3.1).

Lemma 3.1. *We define $w_z^N = u_z^N + \psi_z^N$, where u_z^N and ψ_z^N satisfy (2.3) and (2.2) respectively. Then for the solution u of equation (3.1), we have*

$$-\frac{\partial u}{\partial \bar{\mathbf{n}}}(z, t) = \lim_{N \rightarrow \infty} \int_{\Omega} p(x) w_z^N(x, t) dx.$$

Proof. From the definition of ψ_z^N , we see that $(c^{-1}\partial_t + \mathcal{A})\psi_z^N = 0$. This result and (2.3) show that w_z^N satisfies the equation

$$(c^{-1}\partial_t + \mathcal{A})w_z^N = 0, \quad (x, t) \in \Omega \times (0, T),$$

with the boundary condition $w_z^N|_{\partial\Omega} = \psi_z^N|_{\partial\Omega}$ and the initial condition $w_z^N(x, 0) = 0$. Therefore, Green's identities give that for each $v \in H^1(\Omega)$ with the boundary condition $\mathcal{B}v = 0$,

$$\int_{\Omega} (c^{-1}\partial_t + q)w_z^N(x, t)v(x) + \kappa \nabla w_z^N(x, t) \cdot \nabla v(x) \, dx - \int_{\partial\Omega} \kappa v(x) \frac{\partial w_z^N}{\partial \mathbf{n}}(x, t) \, dx = 0, \quad t \in (0, T).$$

From equation (3.1), we obtain

$$\int_0^t \int_{\Omega} p(x)w_z^N(x, t - \tau) \, dx \, d\tau = \int_0^t \int_{\Omega} (c^{-1}\partial_t + \mathcal{A})u(x, \tau) w_z^N(x, t - \tau) \, dx \, d\tau.$$

Green's identities and the vanishing initial conditions of u and w_z^N give that

$$\begin{aligned} \int_0^t \int_{\Omega} (c^{-1}\partial_t + q)u(x, \tau) w_z^N(x, t - \tau) \, dx \, d\tau &= \int_0^t \int_{\Omega} (c^{-1}\partial_t + q)w_z^N(x, t - \tau) u(x, \tau) \, dx \, d\tau, \\ \int_0^t \int_{\Omega} -\nabla \cdot (\kappa \nabla u(x, \tau)) w_z^N(x, t - \tau) \, dx \, d\tau &= \int_0^t \int_{\Omega} \kappa(x) \nabla u(x, \tau) \cdot \nabla w_z^N(x, t - \tau) \, dx \, d\tau \\ &\quad - \int_0^t \int_{\partial\Omega} \kappa(x) \frac{\partial u}{\partial \mathbf{n}}(x, \tau) w_z^N(x, t - \tau) \, dx \, d\tau. \end{aligned}$$

For the boundary condition of $w_z^N(x)$, we have that

$$\mathcal{B}w_z^N = \sum_{l=1}^N \tilde{\xi}_l(z) \overline{\tilde{\xi}_l(x)}, \quad x \in \partial\Omega.$$

Then it holds that

$$\begin{aligned} &\int_0^t \int_{\partial\Omega} \kappa(x) \frac{\partial u}{\partial \mathbf{n}}(x, \tau) w_z^N(x) \, dx \, d\tau \\ &= \int_0^t \sum_{l=1}^N \tilde{\xi}_l(z) \left\langle \frac{\partial u}{\partial \mathbf{n}}(\cdot, \tau), \tilde{\xi}_l(\cdot) \right\rangle_{\kappa, \partial\Omega} d\tau - \int_0^t \int_{\partial\Omega} \beta \kappa(x) \frac{\partial u}{\partial \mathbf{n}}(x, \tau) \frac{\partial w_z^N}{\partial \mathbf{n}}(x, t - \tau) \, dx \, d\tau \\ &= \int_0^t \sum_{l=1}^N \tilde{\xi}_l(z) \left\langle \frac{\partial u}{\partial \mathbf{n}}(\cdot, \tau), \tilde{\xi}_l(\cdot) \right\rangle_{\kappa, \partial\Omega} d\tau + \int_0^t \int_{\partial\Omega} \kappa(x) u(x, \tau) \frac{\partial w_z^N}{\partial \mathbf{n}}(x, t - \tau) \, dx \, d\tau, \end{aligned}$$

where the boundary condition $\mathcal{B}u = 0$ is used. Hence we have

$$\begin{aligned} &\int_0^t \int_{\Omega} p(x)w_z^N(x, t - \tau) \, dx \, d\tau \\ &= \int_0^t \int_{\Omega} (c^{-1}\partial_t + q)w_z^N(x, t - \tau) u(x, \tau) + \kappa(x) \nabla w_z^N(x, t - \tau) \cdot \nabla u(x, \tau) \, dx \, d\tau \\ &\quad + \int_0^t \int_{\partial\Omega} \kappa(x) u(x, \tau) \frac{\partial w_z^N}{\partial \mathbf{n}}(x, t - \tau) \, dx \, d\tau - \int_0^t \sum_{l=1}^N \tilde{\xi}_l(z) \left\langle \frac{\partial u}{\partial \mathbf{n}}(\cdot, \tau), \tilde{\xi}_l(\cdot) \right\rangle_{\kappa, \partial\Omega} d\tau \end{aligned}$$

$$= - \int_0^t \sum_{l=1}^N \tilde{\xi}_l(z) \left\langle \frac{\partial u}{\partial \mathbf{\tilde{H}}}(\cdot, \tau), \tilde{\xi}_l(\cdot) \right\rangle_{\kappa, \partial\Omega} d\tau.$$

For the above equality, differentiating at time t gives that for $t \in (0, \epsilon)$,

$$- \sum_{l=1}^N \tilde{\xi}_l(z) \left\langle \frac{\partial u}{\partial \mathbf{\tilde{H}}}(\cdot, t), \tilde{\xi}_l(\cdot) \right\rangle_{\kappa, \partial\Omega} = \int_{\Omega} p(x) w_z^N(x, t) dx.$$

From Assumption 2.4 (c) we have for a.e. $t \in (0, \epsilon)$,

$$- \frac{\partial u}{\partial \mathbf{\tilde{H}}}(z, t) = \lim_{N \rightarrow \infty} \int_{\Omega} p(x) w_z^N(x, t) dx.$$

The proof is complete. \square

With the coefficients $\{c_{z,n}\}$ defined in Lemma 2.3, we can deduce the next corollary straightforwardly.

Corollary 3.2. *For a.e. $z \in \partial\Omega$ and $t \in (0, \epsilon)$, it holds that*

$$- \frac{\partial u}{\partial \mathbf{\tilde{H}}}(z, t) = \sum_{n=1}^{\infty} c_{z,n} p_n (1 - e^{-\lambda_n t}),$$

where u is the solution of equation (3.1) and $p_n := \langle p(\cdot), \varphi_n(\cdot) \rangle_{\Omega}$.

Proof. In this proof, let us the limit $\lim_{N \rightarrow \infty} \langle p(\cdot), \overline{w_z^N(\cdot, t)} \rangle_{\Omega}$. Fixing $N \in \mathbb{N}^+$, from the definition of ψ_z^N we have $\psi_z^N \in L^2(\Omega)$. So the Fourier expansion of ψ_z^N can be given as $\psi_z^N = \sum_{n=1}^{\infty} c_{z,n}^N \overline{\varphi_n}$, where $c_{z,n}^N$ is defined in the proof of Lemma 2.3. Moreover, from $w_z^N = u_z^N + \psi_z^N$ and equation (2.3), we have

$$w_z^N(x, t) = \sum_{n=1}^{\infty} c_{z,n}^N (1 - e^{-\lambda_n t}) \overline{\varphi_n(x)}.$$

The above result together with the regularity $\psi_z^N \in L^2(\Omega)$ yields that $w_z^N(\cdot, t) \in L^2(\Omega)$ for $t \in [0, \infty)$. Also recall that $p \in L^2(\Omega)$, then

$$\langle p(\cdot), \overline{w_z^N(\cdot, t)} \rangle_{\Omega} = \sum_{n=1}^{\infty} c_{z,n}^N p_n (1 - e^{-\lambda_n t}).$$

The condition in Assumption 2.4 implies that the Dominated Convergence Theorem can be applied to the above series. So we have

$$\lim_{N \rightarrow \infty} \sum_{n=1}^{\infty} c_{z,n}^N p_n (1 - e^{-\lambda_n t}) = \sum_{n=1}^{\infty} \lim_{N \rightarrow \infty} c_{z,n}^N p_n (1 - e^{-\lambda_n t}).$$

From (2.3), we have

$$\lim_{N \rightarrow \infty} \langle p(\cdot), \overline{w_z^N(\cdot, t)} \rangle_{\Omega} = \lim_{N \rightarrow \infty} \sum_{n=1}^{\infty} c_{z,n}^N p_n (1 - e^{-\lambda_n t}) = \sum_{n=1}^{\infty} c_{z,n} p_n (1 - e^{-\lambda_n t}).$$

The proof is complete. \square

The next two lemmas will be used in the proof of the uniqueness.

Lemma 3.3. *Recall that $\{\lambda_j\}_{j=1}^\infty$ is the set of distinct eigenvalues with increasing order, and the coefficients $\{c_{z,n}\}$ are defined in Lemma 2.3. For any nonempty open subset $\Gamma \subset \partial\Omega$, if*

$$\sum_{\lambda_n=\lambda_j} c_{z,n}\eta_n = 0 \text{ for } j \in \mathbb{N}^+ \text{ and a.e. } z \in \Gamma,$$

then $\{\eta_n\}_{n=1}^\infty = \{0\}$.

Proof. Fixing $j \in \mathbb{N}^+$, from the proof of Lemma 2.3, we have

$$\begin{aligned} c_{z,n} &= \lambda_j^{-1} \lim_{N \rightarrow \infty} \langle \psi_z^N, \mathcal{A}\overline{\varphi_n} \rangle_\Omega \\ &= \lambda_j^{-1} \lim_{N \rightarrow \infty} \left(\langle \mathcal{A}\psi_z^N, \overline{\varphi_n} \rangle_\Omega - \langle \psi_z^N, \frac{\partial \overline{\varphi_n}}{\partial \overline{\mathbf{n}}} \rangle_{\kappa, \partial\Omega} + \langle \frac{\partial \psi_z^N}{\partial \overline{\mathbf{n}}}, \overline{\varphi_n} \rangle_{\kappa, \partial\Omega} \right) \\ &= -\lambda_j^{-1} \sum_{l=1}^\infty \tilde{\xi}_l(z) \langle \frac{\partial \varphi_n}{\partial \overline{\mathbf{n}}}, \tilde{\xi}_l \rangle_{\kappa, \partial\Omega}. \end{aligned}$$

With the definition of the orthonormal basis $\{\tilde{\xi}_l\}_{l=1}^\infty$, the above series is actually finite. This gives that for a.e. $z \in \Gamma$,

$$\sum_{l=1}^\infty \tilde{\xi}_l(z) \langle \frac{\partial \varphi_n}{\partial \overline{\mathbf{n}}}, \tilde{\xi}_l \rangle_{\kappa, \partial\Omega} = \frac{\partial \varphi_n}{\partial \overline{\mathbf{n}}}(z),$$

which leads to $\sum_{\lambda_n=\lambda_j} \eta_n \frac{\partial \varphi_n}{\partial \overline{\mathbf{n}}}(z) = 0$ for a.e. $z \in \Gamma$. Assume that $\{\eta_n : \lambda_n = \lambda_j\} \neq \{0\}$, then the linear independence of the set $\{\varphi_n(x) : \lambda_n = \lambda_j\}$ yields that $\sum_{\lambda_n=\lambda_j} \eta_n \varphi_n(x)$ is not vanishing on Ω . However, we see that $\sum_{\lambda_n=\lambda_j} \eta_n \varphi_n(x)$ is an eigenfunction corresponding to the eigenvalue λ_j . These and Lemma 2.1 give that $\sum_{\lambda_n=\lambda_j} \eta_n \frac{\partial \varphi_n}{\partial \overline{\mathbf{n}}}$ can not vanish almost everywhere on Γ , which is a contradiction. Hence, we prove that $\{\eta_n : \lambda_n = \lambda_j\} = \{0\}$ for each $j \in \mathbb{N}^+$, namely, $\eta_n = 0$ for $n \in \mathbb{N}^+$. The proof is complete. \square

Lemma 3.4. *Set $\Gamma \subset \partial\Omega$ be a nonempty open subset and let $\sum_{n=1}^\infty c_{z,n}\eta_n$ be absolute convergent for a.e. $z \in \Gamma$. Then the result*

$$\sum_{n=1}^\infty c_{z,n}\eta_n(1 - e^{-\lambda_n t}) = 0 \text{ for } t \in (0, \epsilon) \text{ and a.e. } z \in \Gamma$$

implies that $\eta_n = 0$ for $n \in \mathbb{N}^+$.

Proof. From [34, Lemma 3.5] we have that $\sum_{\lambda_n=\lambda_j} c_{z,n}\eta_n = 0$ for each $j \in \mathbb{N}^+$ and a.e. $z \in \Gamma$. Then Lemma 3.3 gives the desired result and completes the proof. \square

The next proposition concerns with the uniqueness result of equation (3.1).

Proposition 3.5. *For the PDE (3.1), the data $\frac{\partial u}{\partial \overline{\mathbf{n}}} \big|_{\Gamma \times (0, \epsilon)}$ can uniquely determine $p(x)$.*

Proof. Given $p(x)$ and $\tilde{p}(x)$, we set u and \tilde{u} be the corresponding solutions of equation (3.1) with p and \tilde{p} respectively. If $\frac{\partial u}{\partial \mathbf{n}}|_{\Gamma \times (0, \epsilon)} = \frac{\partial \tilde{u}}{\partial \mathbf{n}}|_{\Gamma \times (0, \epsilon)}$, we need to show that $\|p - \tilde{p}\|_{L^2(\Omega)} = 0$.

From Corollary 3.2, we have

$$\sum_{n=1}^{\infty} c_{z,n}(p_n - \tilde{p}_n)(1 - e^{-\lambda_n t}) = 0, \quad t \in (0, \epsilon).$$

Then by Lemma 3.4, we conclude that $p_n = \tilde{p}_n$ for $n \in \mathbb{N}^+$. This leads to the desired result and completes the proof. \square

Now we can state the uniqueness theorem of the inverse problem (1.6).

Theorem 1. *For equation (1.2), the data (1.4) can uniquely determine the source (1.5).*

More precisely, given two sets of unknown $\{p_k(x)\}_{k=1}^K$ and $\{\tilde{p}_k(x)\}_{k=1}^K$, we denote the corresponding solutions of equation (1.2) by u_m and \tilde{u}_m respectively. Providing

$$\frac{\partial u_m}{\partial \mathbf{n}}|_{\Gamma \times (0, T)} = \frac{\partial \tilde{u}_m}{\partial \mathbf{n}}|_{\Gamma \times (0, T)},$$

it holds that

$$p_k = \tilde{p}_k \text{ in } L^2(\Omega) \text{ for } k = 1, \dots, K.$$

Proof. From equation (1.2), if we restrict $t^* \in (0, t_1)$, then we can give the models of $u(x, t^*)$ and $\tilde{u}(x, t^*)$ as follows:

$$\begin{cases} (c^{-1}\partial_t + \mathcal{A})u(x, t^*) = p_1(x), & (x, t^*) \in \Omega \times (0, t_1), \\ u(x, t^*) = 0, & (x, t^*) \in \partial\Omega \times (0, t_1) \cup \Omega \times \{0\}, \end{cases}$$

and

$$\begin{cases} (c^{-1}\partial_t + \mathcal{A})\tilde{u}(x, t^*) = \tilde{p}_1(x), & (x, t^*) \in \Omega \times (0, t_1), \\ \tilde{u}(x, t^*) = 0, & (x, t^*) \in \partial\Omega \times (0, t_1) \cup \Omega \times \{0\}. \end{cases}$$

From Proposition 3.5, we have that $p_1 = \tilde{p}_1$ in the sense of $L^2(\Omega)$, which also gives that $u(x, t_1) = \tilde{u}(x, t_1)$.

After that, by setting $t^* = t - t_1$ and $t^* \in (0, t_2 - t_1)$, we have

$$\begin{cases} (c^{-1}\partial_t + \mathcal{A})u(x, t^*) = p_2(x), & (x, t^*) \in \Omega \times (0, t_2 - t_1), \\ u(x, 0) = u(x, t_1), & x \in \Omega, \\ u(x, t^*) = 0, & (x, t^*) \in \partial\Omega \times (0, t_2 - t_1), \end{cases}$$

and

$$\begin{cases} (c^{-1}\partial_t + \mathcal{A})\tilde{u}(x, t^*) = \tilde{p}_1(x), & (x, t^*) \in \Omega \times (0, t_2 - t_1), \\ \tilde{u}(x, 0) = u(x, t_1), & x \in \Omega, \\ u(x, t^*) = 0, & (x, t^*) \in \partial\Omega \times (0, t_2 - t_1). \end{cases}$$

Next, if we set $w = u - u(x, t_1)$ and $\tilde{w} = \tilde{u} - u(x, t_1)$, we have that

$$\begin{cases} (c^{-1}\partial_t + \mathcal{A})w(x, t^*) = p_2(x) - \mathcal{A}u(x, t_1), & (x, t^*) \in \Omega \times (0, t_2 - t_1), \\ w(x, t^*) = 0, & (x, t^*) \in \partial\Omega \times (0, t_2 - t_1) \cup \Omega \times \{0\}, \end{cases}$$

and

$$\begin{cases} (c^{-1}\partial_t + \mathcal{A})\tilde{w}(x, t^*) = \tilde{p}_2(x) - \mathcal{A}u(x, t_1), & (x, t^*) \in \Omega \times (0, t_2 - t_1), \\ \tilde{w}(x, t^*) = 0, & (x, t^*) \in \partial\Omega \times (0, t_2 - t_1) \cup \Omega \times \{0\}. \end{cases}$$

From Proposition 3.5, we have that $p_2 = \tilde{p}_2$ and $u(x, t_2) = \tilde{u}(x, t_2)$.

Continuing this argument, we can achieve the desired result and complete the proof. \square

3.2 Conditional stability of Lipschitz type

We next consider the Lipschitz stability for our inverse problem of recovering $\{p_k(x)\}_{k=1}^K$ in (1.5) from the boundary data (1.4). Similar as done in [40, 39], the crucial point is to construct an integral identity connecting the inversion input data with the unknown functions.

We introduce the adjoint problem of (1.2) as

$$\begin{cases} (-c^{-1}\partial_t + \mathcal{A})\phi(x, t) = 0, & x \in \Omega, \ t \in (0, T), \\ \phi(x, T) = 0, & x \in \Omega, \\ \mathcal{B}\phi = \begin{cases} \omega(x, t), & x \in \Gamma, \ t \in (0, T), \\ 0, & x \in \partial\Omega \setminus \Gamma, \ t \in (0, T). \end{cases} \end{cases} \quad (3.2)$$

Then the following lemma gives a variational identity.

Lemma 3.6. *Let Γ be a nonempty open subset of boundary $\partial\Omega$. For the given time mesh $\{t_k\}_{k=0}^K$ with $t_K = T$, we denote u_m and \tilde{u}_m as the solution of equation (1.2) with*

$$S[\mu_f, u_e] = \sum_{k=1}^K p_k(x) \chi_{t \in [t_{k-1}, t_k)} \text{ and } \tilde{S}[\tilde{\mu}_f, u_e] = \sum_{k=1}^K \tilde{p}_k(x) \chi_{t \in [t_{k-1}, t_k)}$$

respectively. Then there holds that

$$\sum_{k=1}^K \int_{t_{k-1}}^{t_k} \int_{\Omega} (p_k - \tilde{p}_k)(x) \phi[\omega](x, t) \, dx \, dt = \int_0^T \int_{\Gamma} \omega(x, t) \left(\frac{\partial u_m}{\partial \mathbf{n}} - \frac{\partial \tilde{u}_m}{\partial \mathbf{n}} \right) \, dx \, dt, \quad (3.3)$$

where $\phi[\omega]$ is the solution to (3.2) for $\omega \in L^2(\Gamma \times (0, T))$.

Proof. We see that $U_m := u_m - \tilde{u}_m$ satisfies

$$\begin{cases} (c^{-1}\partial_t + \mathcal{A}) U_m(x, t) = \sum_{k=1}^K (p_k - \tilde{p}_k)(x) \chi_{t \in [t_{k-1}, t_k)}, & (x, t) \in \Omega \times (0, T), \\ U_m(x, 0) = 0, & x \in \Omega, \\ \mathcal{B}U_m = 0, & (x, t) \in \partial\Omega \times (0, T). \end{cases} \quad (3.4)$$

Multiplying $\phi(x, t) := \phi[\omega](x, t)$ on the two sides of equation (3.4) and integrating them in $\Omega \times (0, T)$, we get

$$\int_0^T \int_{\Omega} (c^{-1}\partial_t + \mathcal{A}) U_m(x, t) \phi(x, t) \, dx \, dt = \sum_{k=1}^K \int_{t_{k-1}}^{t_k} \int_{\Omega} (p_k - \tilde{p}_k)(x) \phi[\omega](x, t) \, dx \, dt. \quad (3.5)$$

By $\phi(x, T) = 0$, $U_m(x, 0) = 0$ and $\{\phi, U_m\} \subset L^2(0, T; H^2(\Omega))$, we have

$$\begin{aligned} \int_0^T \int_{\Omega} (c^{-1} \partial_t U_m) \phi \, dx \, dt &= \int_{\Omega} (U_m \phi)|_{t=0}^{t=T} \, dx - \int_0^T \int_{\Omega} U_m (c^{-1} \partial_t \phi) \, dx \, dt \\ &= - \int_0^T \int_{\Omega} U_m (c^{-1} \partial_t \phi) \, dx \, dt. \end{aligned} \quad (3.6)$$

The Green formula also gives that

$$\begin{aligned} \int_0^T \int_{\Omega} (\mathcal{A} U_m) \phi \, dx \, dt &= \int_0^T \int_{\Omega} (\mathcal{A} \phi) U_m \, dx \, dt \\ &\quad + \int_0^T \int_{\partial \Omega} \left(\phi \frac{\partial U_m}{\partial \vec{\mathbf{n}}} - U_m \frac{\partial \phi}{\partial \vec{\mathbf{n}}} \right) \, dx \, dt. \end{aligned} \quad (3.7)$$

Combining (3.5)-(3.7) together and using (3.2), we finally have

$$\begin{aligned} \sum_{k=1}^K \int_{t_{k-1}}^{t_k} \int_{\Omega} (p_k - \tilde{p}_k)(x) \phi[\omega](x, t) \, dx \, dt &= \int_0^T \int_{\partial \Omega} \left(\phi \frac{\partial U_m}{\partial \vec{\mathbf{n}}} - U_m \frac{\partial \phi}{\partial \vec{\mathbf{n}}} \right) \, dx \, dt \\ &= \int_0^T \int_{\partial \Omega} (\mathcal{B} \phi) \frac{\partial U_m}{\partial \vec{\mathbf{n}}} \, dx \, dt. \end{aligned}$$

Henceforth, utilizing the boundary condition

$$\mathcal{B} \phi = \begin{cases} \omega(x, t), & x \in \Gamma, \, t \in (0, T), \\ 0, & x \in \partial \Omega \setminus \Gamma, \, t \in (0, T), \end{cases}$$

we deduce the desired result and complete the proof. \square

For the set of functions $\{p_k(x)\}_{k=1}^K$, we use the related vector form as $\vec{p} := (p_1, \dots, p_K)$ and define the operator $L : (L^2(\Omega))^K \rightarrow L^2(\Omega \times (0, T))$ as

$$L\vec{p} = \sum_{k=1}^K p_k(x) \chi_{t \in [t_{k-1}, t_k]}.$$

Next we give a bilinear functional with respect to $L\vec{p}$ and $\omega(x, t)$ by

$$\mathcal{L}(L\vec{p}, \omega) = \int_{\Omega \times (0, T)} (L\vec{p})(x, t) \phi[\omega](x, t) \, dx \, dt, \quad (3.8)$$

where $\phi[\omega](x, t)$ satisfies (3.2). The corresponding norm $\|\cdot\|_{\mathcal{L}}$ is introduced in the following lemma.

Lemma 3.7. *With (3.8), we define the function $\|\cdot\|_{\mathcal{L}} : l^1((L^2(\Omega))^K) \rightarrow \mathbb{R}$ as*

$$\|\vec{p}\|_{\mathcal{L}} := \sup_{\omega \in W} \frac{|\mathcal{L}(L\vec{p}, \omega)|}{\|\omega\|_{L^2(\Gamma \times (0, T))}}, \quad (3.9)$$

where

$$W := \{\psi : \psi \in L^2(\Gamma \times (0, T)), \, \psi \not\equiv 0\}.$$

Then $\|\cdot\|_{\mathcal{L}}$ is a norm on $l^1((L^2(\Omega))^K)$.

Proof. Firstly, let us prove the well-definedness of $\|\vec{p}\|_{\mathcal{L}}$. With Holder inequality, we have

$$\begin{aligned} |\mathcal{L}(L\vec{p}, \omega)| &\leq \sum_{k=1}^K \int_{t_{k-1}}^{t_k} \int_{\Omega} |p_k(x) \phi[\omega](x, t)| \, dx \, dt \\ &\leq \sum_{k=1}^K \|p_k\|_{L^2(\Omega)} \|\phi[\omega]\|_{L^2(\Omega \times (t_{k-1}, t_k))} \leq C \|\omega\|_{L^2(0, T; \Gamma)} \sum_{k=1}^K \|p_k\|_{L^2(\Omega)} \\ &\leq C \sum_{k=1}^K \|\omega\|_{L^2(t_{k-1}, t_k; \Gamma)} \|p_k\|_{L^2(\Omega)} \leq C \|\omega\|_{L^2(0, T; \Gamma)} \sum_{k=1}^K \|p_k\|_{L^2(\Omega)}, \end{aligned}$$

which gives

$$\frac{|\mathcal{L}(L\vec{p}, \omega)|}{\|\omega\|_{L^2(\Gamma \times (0, T))}} \leq C \sum_{k=1}^K \|p_k\|_{L^2(\Omega)} = C \|\vec{p}\|_{l^1((L^2(\Omega))^K)}, \quad \omega \in W.$$

So we have $\|\vec{p}\|_{\mathcal{L}} \leq C \|\vec{p}\|_{l^1((L^2(\Omega))^K)} < \infty$.

Next we prove that $\|\cdot\|_{\mathcal{L}}$ is a norm on $l^1((L^2(\Omega))^K)$. Firstly, it is obviously that

$$\|\vec{p}\|_{\mathcal{L}} \geq 0 \text{ and } \|c\vec{p}\|_{\mathcal{L}} = |c| \|\vec{p}\|_{\mathcal{L}} \text{ for } c \in \mathbb{R} \text{ and } \vec{p} \in l^1((L^2(\Omega))^K).$$

Secondly, from the definition of $\|\cdot\|_{\mathcal{L}}$, we can prove that

$$\begin{aligned} \|\vec{p}_1 + \vec{p}_2\|_{\mathcal{L}} &= \sup_{\omega \in W} \frac{|\mathcal{L}(L\vec{p}_1 + L\vec{p}_2, \omega)|}{\|\omega\|_{L^2(\Gamma \times (0, T))}} \leq \sup_{\omega \in W} \frac{|\mathcal{L}(L\vec{p}_1, \omega)| + |\mathcal{L}(L\vec{p}_2, \omega)|}{\|\omega\|_{L^2(\Gamma \times (0, T))}} \\ &\leq \sup_{\omega \in W} \frac{|\mathcal{L}(L\vec{p}_1, \omega)|}{\|\omega\|_{L^2(\Gamma \times (0, T))}} + \sup_{\omega \in W} \frac{|\mathcal{L}(L\vec{p}_2, \omega)|}{\|\omega\|_{L^2(\Gamma \times (0, T))}} = \|\vec{p}_1\|_{\mathcal{L}} + \|\vec{p}_2\|_{\mathcal{L}}, \end{aligned}$$

which is the triangle inequality. At last, we need to show that $\|\vec{p}\|_{\mathcal{L}} = 0$ leads to $\vec{p} = 0$. Given $\|\vec{p}\|_{\mathcal{L}} = 0$, we have that $|\mathcal{L}(L\vec{p}, \omega)| = 0$ for each $\omega \in W$. This together with Lemma 3.6 yields that

$$\int_0^T \int_{\Gamma} \omega(x, t) \frac{\partial u_m}{\partial \vec{\mathbf{n}}} \, dx \, dt = 0, \quad \forall \omega \in L^2(\Gamma \times (0, T)),$$

which leads to $\frac{\partial u_m}{\partial \vec{\mathbf{n}}} = 0$ in $L^2(\Gamma \times (0, T))$. Then by Theorem 1, we deduce that $p_k = 0$ in $L^2(\Omega)$ for $k = 1, \dots, K$, i.e., $\vec{p} = 0$. Now we have proved that $\|\cdot\|_{\mathcal{L}}$ is a norm on $l^1((L^2(\Omega))^K)$ and the proof is complete. \square

Now we can establish the conditional stability of Lipschitz type for the inverse problem by the weighted norm $\|\cdot\|_{\mathcal{L}}$.

Theorem 2. We set Γ to be a nonempty open subset of boundary $\partial\Omega$, and denote the solutions of (1.2) with $\vec{p} = (p_1, \dots, p_K)$ and $\vec{\tilde{p}} = (\tilde{p}_1, \dots, \tilde{p}_K)$ by u_m and \tilde{u}_m respectively. Then the next stability result holds

$$\|\vec{p} - \vec{\tilde{p}}\|_{\mathcal{L}} \leq \left\| \frac{\partial u_m}{\partial \vec{\mathbf{n}}} - \frac{\partial \tilde{u}_m}{\partial \vec{\mathbf{n}}} \right\|_{L^2(\Gamma \times (0, T))}.$$

Proof. By (3.3) and the definition (3.9), we have

$$\begin{aligned}\|\vec{p} - \vec{\tilde{p}}\|_{\mathcal{L}} &= \sup_{\omega \in W} \frac{|\mathcal{L}(L(\vec{p} - \vec{\tilde{p}}), \omega)|}{\|\omega\|_{L^2(\Gamma \times (0, T))}} \\ &= \sup_{\omega \in W} \|\omega\|_{L^2(\Gamma \times (0, T))}^{-1} \left| \int_0^T \int_{\Gamma} \omega(x, t) \left(\frac{\partial u_m}{\partial \vec{\mathbf{n}}} - \frac{\partial \tilde{u}_m}{\partial \vec{\mathbf{n}}} \right) dx dt \right|.\end{aligned}$$

With Cauchy-Schwartz inequality, we immediately deduce that

$$\|\vec{p} - \vec{\tilde{p}}\|_{\mathcal{L}} \leq \left\| \frac{\partial u_m}{\partial \vec{\mathbf{n}}} - \frac{\partial \tilde{u}_m}{\partial \vec{\mathbf{n}}} \right\|_{L^2(\Gamma \times (0, T))}.$$

The proof is complete. \square

4 Generalization error estimates.

In this section, we introduce the proposed reconstruction scheme with its associated error estimates. This lays the foundations of our approach that we subsequently test numerically. We decompose this inverse problem (1.6) into solving a forward problem to get u_e and an inverse problem for recovering (μ_f, u_m) . More precisely, we solve the forward problem (1.1) with the known boundary input to obtain $u_e(x, t)$, and then reconstruct μ_f and u_m from the observation data (1.4) with the obtained solution u_e .

4.1 Loss functions.

We assume that the activation function is of C^2 regularity. This includes activation such as $\sigma = \tanh$. Then, for the neural network $u_{e, \theta_e}, u_{m, \theta_m}$ defined by (2.4) in terms of σ , we set $u_{e, \theta_e}, u_{m, \theta_m} \in C^l(\overline{\Omega} \times [0, T])$ for $l = 0, 1, 2$. For the network parameters $\theta_e, \theta_m \in \Theta := \{ \{(W_k, b_k)\}_{k=1}^K : W_k \in \mathbb{R}^{d_k \times d_{k-1}}, b_k \in \mathbb{R}^{d_k} \}$, the set of all possible trainable parameters, $u_{e, \theta_e}(x, t), u_{m, \theta_m}(x, t)$ up to second order derivatives are bounded in $\overline{\Omega} \times [0, T]$ for any specified θ_e, θ_m .

For given boundary input, it is necessary to solve the forward problem (1.1) first. We denote the approximate solution of (1.1) is u_{e, θ_e} , which is a deep neural networks function with the networks parameters θ_e . Next the following residuals for the forward problem (1.1) are introduced.

- Interior PDE residual

$$\mathcal{R}_{int, \theta_e}(x, t) := (c^{-1} \partial_t + \mathcal{A}) u_{e, \theta_e}(x, t), \quad (x, t) \in \Omega \times (0, T).$$

- Spatial boundary residual

$$\mathcal{R}_{sb, \theta_e}(x, t) := \mathcal{B} u_{e, \theta_e}(x, t) - \mathcal{B} u_e(x, t), \quad (x, t) \in \partial\Omega \times (0, T).$$

- Temporal boundary (initial status) residual

$$\mathcal{R}_{tb, \theta_e}(x) := u_{e, \theta_e}(x, 0), \quad x \in \Omega.$$

We minimize the following loss function

$$J_1(\theta_e) = \|\mathcal{R}_{int,\theta_e}\|_{L^2(0,T;L^2(\Omega))} + \|\mathcal{R}_{tb,\theta_e}\|_{L^2(\Omega)} + \|\mathcal{R}_{sb,\theta_e}\|_{L^2(0,T;L^2(\partial\Omega))} \quad (4.1)$$

to search for the optimal parameters θ_e^* . The obtained $u_e^*(x, t) := u_{e,\theta_e^*}(x, t)$ can be regarded as approximate solution of the forward problem (1.1).

Next, we introduce a form loss function of data-driven solution of inverse problems that ensures reconstruction accuracy owing to the conditional stability of the inverse problem. For this purpose, we need to define suitable residuals measuring the errors of the governed system and the input data. Define the following residuals for the emission system.

- Interior PDE residual

$$\mathcal{R}_{int,\theta_m,\theta_f,\theta_e^*}(x, t) := (c^{-1}\partial_t + \mathcal{A})u_{m,\theta_m}(x, t) - \mu_{f,\theta_f}(x, t)u_{e,\theta_e^*}(x, t; x_s), \quad (x, t) \in \Omega \times (0, T).$$

- Spatial boundary residual

$$\mathcal{R}_{sb,\theta_m}(x, t) := \mathcal{B}u_{m,\theta_m}(x, t), \quad (x, t) \in \partial\Omega \times (0, T).$$

- Temporal boundary (initial status) residual

$$\mathcal{R}_{tb,\theta_m}(x) := u_{m,\theta_m}(x, 0), \quad x \in \Omega.$$

- Data residual

$$\mathcal{R}_{d,\theta_m}(x, t) := \frac{\partial u_{m,\theta_m}}{\partial \mathbf{H}} - \varphi^\delta(x, t), \quad (x, t) \in \Gamma \times (0, T).$$

Thus, a loss function minimization scheme seeks to minimize these residuals comprehensively with some weights balancing different residuals. We define a new loss function involving the norm of the derivatives for some residuals, namely

$$J_2(\theta_f, \theta_m) = \lambda \|\mathcal{R}_{d,\theta_m}\|_{L^2(\Gamma \times (0,T))} + \|\mathcal{R}_{int,\theta_m,\theta_f,\theta_e^*}\|_{L^2(0,T;L^2(\Omega))} + \|\mathcal{R}_{tb,\theta_m}\|_{H_0^1(\Omega)} + \|\mathcal{R}_{sb,\theta_m}\|_{H^1(0,T;H^1(\partial\Omega))}, \quad (4.2)$$

where λ is a hyper-parameter to balance the residuals between the knowledge of PDE and the measurement data.

To evaluate the integrals in (4.1) and (4.2) numerically, we introduce the training sets

$$\begin{aligned} \mathcal{S}_d &:= \{(x_n, t_n) : (x_n, t_n) \in \Gamma \times (0, T], \quad n = 1, 2, \dots, N_d\}, \\ \mathcal{S}_{int} &:= \{(\tilde{x}_n, \tilde{t}_n) : (\tilde{x}_n, \tilde{t}_n) \in \Omega_T, \quad n = 1, 2, \dots, N_{int}\}, \\ \mathcal{S}_{tb} &:= \{(\bar{x}_n, 0) : \bar{x}_n \in \Omega, \quad n = 1, 2, \dots, N_{tb}\}, \\ \mathcal{S}_{sb} &:= \{(\hat{x}_n, \hat{t}_n) : (\hat{x}_n, \hat{t}_n) \in \partial\Omega_T, \quad n = 1, 2, \dots, N_{sb}\}. \end{aligned}$$

Applying these sets and the numerical quadrature rules [31], we can consider the following two empirical loss function

$$J_1^N(\theta_e) = \sum_{n=1}^{\bar{N}_{int}} \bar{\omega}_n^{int} \left| \mathcal{R}_{int,\theta_e}(\tilde{x}_n, \tilde{t}_n) \right|^2 + \sum_{n=1}^{\bar{N}_{tb}} \bar{\omega}_n^{tb} \left| \mathcal{R}_{tb,\theta_e}(\bar{x}_n) \right|^2 + \sum_{n=1}^{\bar{N}_{sb}} \bar{\omega}_n^{sb} \left| \mathcal{R}_{sb,\theta_e}(\hat{x}_n, \hat{t}_n) \right|^2, \quad (4.3)$$

and

$$\begin{aligned}
J_2^N(\theta_f, \theta_m) = & \lambda \sum_{n=1}^{N_d} \omega_n^d \left| \mathcal{R}_{d, \theta_m}(x_n, t_n) \right|^2 + \sum_{n=1}^{N_{int}} \omega_n^{int} \left| \mathcal{R}_{int, \theta_f, \theta_m, \theta_e^*}(\tilde{x}_n, \tilde{t}_n) \right|^2 \\
& + \sum_{n=1}^{N_{tb}} \omega_n^{tb,0} \left| \mathcal{R}_{tb, \theta_m}(\bar{x}_n) \right|^2 + \sum_{n=1}^{N_{tb}} \omega_n^{tb,1} \left| \partial_t \mathcal{R}_{tb, \theta_m}(\bar{x}_n) \right|^2 \\
& + \sum_{n=1}^{N_{sb}} \omega_n^{sb,0} \left| \mathcal{R}_{sb, \theta}(\hat{x}_n, \hat{t}_n) \right|^2 + \sum_{n=1}^{N_{sb}} \omega_n^{sb,1} \left| \frac{\partial \mathcal{R}_{sb, \theta}}{\partial \vec{\mathbf{n}}}(\hat{x}_n, \hat{t}_n) \right|^2 \\
& + \sum_{n=1}^{N_{sb}} \omega_n^{sb,2} \left| \frac{\partial \mathcal{R}_{sb, \theta}}{\partial t}(\hat{x}_n, \hat{t}_n) \right|^2 + \sum_{n=1}^{N_{sb}} \omega_n^{sb,3} \left| \frac{\partial^2 \mathcal{R}_{sb, \theta}}{\partial t \partial \vec{\mathbf{n}}}(\hat{x}_n, \hat{t}_n) \right|^2,
\end{aligned} \tag{4.4}$$

where the coefficients $\bar{\omega}_n^{int}$, $\bar{\omega}_n^{tb}$, $\bar{\omega}_n^{sb}$, ω_n^d , ω_n^{int} , $\omega_n^{tb,k}$, $\omega_n^{sb,j}$ with $k = 0, 1$ and $j = 0, 1, 2, 3$ are the quadrature weights. Applying the quadrature rules (2.5), it is easy to see that the error for the loss function is

$$\begin{aligned}
|J_1(\theta_e) - J_1^N(\theta_e)| & \leq C \max\{\bar{N}_{int}^{-\bar{\alpha}_{int}}, \bar{N}_{tb}^{-\bar{\alpha}_{tb}}, \bar{N}_{sb}^{-\bar{\alpha}_{sb}}\}, \\
|J_2(\theta_f, \theta_m) - J_2^N(\theta_f, \theta_m)| & \leq C \max_{k=0,1, j=0,1,2,3} \{N_d^{-\alpha_d}, N_{int}^{-\alpha_{int}}, N_{tb}^{-\alpha_{tb,k}}, N_{sb}^{-\alpha_{sb,j}}\},
\end{aligned} \tag{4.5}$$

where C depends on the continuous norm $\|\cdot\|_{C(\Omega)}$ of the integrands. Therefore, the underlying solutions and neural networks have to be sufficiently regular such that the residuals can be approximated to high accuracy by the quadrature rules.

4.2 The estimates of generalization error.

We give the regularity estimate of the PDEs with non-homogenous boundary condition. The following L^p estimate on elliptic system can be found in reference [1].

Lemma 4.1. *Let $w(x) \in H^2(\Omega)$ solve*

$$\begin{cases} -\Delta w = f(x), & x \in \Omega, \\ \frac{\partial w}{\partial \vec{\mathbf{n}}} + \beta w = b(x), & x \in \partial\Omega, \end{cases}$$

for $0 < \beta_0 \leq \beta(x) \in C(\partial\Omega)$. Then we have

$$\|w\|_{H^2(\Omega)} \leq C(\|f\|_{L^2(\Omega)} + \|\tilde{b}\|_{H^1(\Omega)}) \leq C(\|f\|_{L^2(\Omega)} + \|b\|_{H^{1/2}(\partial\Omega)}),$$

where $\tilde{b}(x) \in H^1(\Omega)$ is the extension of $b(x) \in H^{1/2}(\partial\Omega)$.

Lemma 4.2. *Consider the following PDEs with non-homogenous boundary condition*

$$\begin{cases} (c^{-1}\partial_t + \mathcal{A})V(x, t) = 0, & (x, t) \in \Omega \times (0, T), \\ V(x, 0) = 0, & x \in \Omega, \\ \mathcal{B}V(x, t) = B(x, t), & (x, t) \in \partial\Omega \times (0, T), \end{cases} \tag{4.6}$$

if the boundary condition $B \in H^1(0, T; H^{1/2}(\partial\Omega))$, then there exists a unique solution $V \in L^2(0, T; H^2(\Omega))$ with the estimate

$$\|V\|_{L^2(0, T; H^2(\Omega))} \leq C\|B\|_{H^1(0, T; H^{1/2}(\partial\Omega))}.$$

Proof. For any fixed $t \in [0, T]$, define $\Lambda_b(x, t)$ from

$$\begin{cases} -\mathcal{A}\Lambda_b(x, t) = 0, & x \in \Omega, \\ \mathcal{B}\Lambda_b(x, t) = B(x, t), & x \in \partial\Omega. \end{cases} \quad (4.7)$$

By the regularity estimate on elliptic problem and Lemma 4.1, there exists a unique solution $\Lambda_b(\cdot, t) \in H^2(\Omega)$ satisfying $\|\Lambda_b(\cdot, t)\|_{H^2(\Omega)} \leq C_t \|\tilde{B}(\cdot, t)\|_{H^1(\Omega)}$. Since $\beta(x)$ is independent of t , we also have for $k = 0, 1, 2$ that

$$\|\partial_t^k \Lambda_b(\cdot, t)\|_{H^2(\Omega)} \leq C \|\partial_t^k \tilde{B}(\cdot, t)\|_{H^1(\Omega)} \leq C \|\partial_t^k B(\cdot, t)\|_{H^{1/2}(\partial\Omega)}, \quad t \in [0, T].$$

Let $AC[0, T]$ be the space of absolutely continuous functions. For $B(x, \cdot) \in AC[0, T]$, it follows $\Lambda_b(x, \cdot) \in AC[0, T]$ by (4.7). So we can decompose $V = V_c + \Lambda_b$, where V_c satisfies

$$\begin{cases} (c^{-1} \partial_t + \mathcal{A})V_c(x, t) = -c^{-1} \partial_t \Lambda_b, & (x, t) \in \Omega \times (0, T), \\ \mathcal{B}V_c(x, t) = 0, & (x, t) \in \partial\Omega \times [0, T], \\ V_c(x, 0) = -\Lambda_b(x, 0) = 0, & x \in \Omega. \end{cases}$$

From the regularity estimates in [12], there holds

$$\|V_c\|_{L^2(0, T; H^2(\Omega))} \leq C \|\partial_t \Lambda_b\|_{L^2(0, T; L^2(\Omega))} \leq C \|\partial_t B\|_{L^2(0, T; H^{1/2}(\partial\Omega))}.$$

Sequentially, we have

$$\begin{aligned} \|V\|_{L^2(0, T; H^2(\Omega))} &\leq \|\Lambda_b\|_{L^2(0, T; H^2(\Omega))} + \|V_c\|_{L^2(0, T; H^2(\Omega))} \\ &\leq C(\|B\|_{L^2(0, T; H^{1/2}(\partial\Omega))} + \|\partial_t B\|_{L^2(0, T; H^{1/2}(\partial\Omega))}) \\ &\leq C\|B\|_{H^1(0, T; H^{1/2}(\partial\Omega))}. \end{aligned}$$

The proof is complete. \square

Now, we define the generalization errors as

$$\begin{cases} \mathcal{E}_{G, u_e} := \|u_e^* - u_{e, ex}\|_{C([0, T]; L^2(\Omega))}, \\ \mathcal{E}_{G, \vec{p}} := \|\vec{p}_* - \vec{p}_{ex}\|_{\mathcal{L}}, \\ \mathcal{E}_{G, u_m} := \|u_m^* - u_{m, ex}\|_{C([0, T]; L^2(\Omega))}, \end{cases} \quad (4.8)$$

where $(u_e^*, u_m^*, \mu_f^*) := (u_{e, \theta_e^*}, u_{m, \theta_m^*}, \mu_{f, \theta_f^*})$ with the minimizer $(\theta_e^*, \theta_m^*, \theta_f^*)$ of functional (4.3) and (4.4). They can be used to approximate the exact solution $(u_{e, ex}, u_{m, ex}, \mu_{f, ex})$ of the inverse problem (1.6). The related vector forms are given as $\vec{p}_* := (p_1^*, \dots, p_K^*)$ and $\vec{p}_{ex} := (p_{1, ex}, \dots, p_{K, ex})$, which are the approximate networks solution corresponding to $\mu_f^* u_e^*$ and exact $\mu_{f, ex} u_{e, ex}$, respectively. We will estimate the generalization errors in terms of the training errors for both excitation and emission, which are given below.

Define the training errors for excitation process:

- The interior PDE training errors

$$\bar{\mathcal{E}}_{T, int} := \left(\sum_{n=1}^{\bar{N}_{int}} \bar{\omega}_n^{int} \left| \mathcal{R}_{int, \theta_e^*}(\tilde{x}_n, \tilde{t}_n) \right|^2 \right)^{1/2}.$$

- The initial condition training errors

$$\bar{\mathcal{E}}_{T,tb} := \left(\sum_{n=1}^{\bar{N}_{tb}} \bar{\omega}_n^{tb} \left| \mathcal{R}_{tb,\theta_e^*}(\bar{x}_n) \right|^2 \right)^{1/2}.$$

- The spatial boundary condition training errors

$$\bar{\mathcal{E}}_{T,sb} := \left(\sum_{n=1}^{\bar{N}_{sb}} \bar{\omega}_n^{sb} \left| \mathcal{R}_{sb,\theta_e^*}(\hat{x}_n, \hat{t}_n) \right|^2 \right)^{1/2}.$$

Define the training errors for emission process:

- The measurement data training errors

$$\mathcal{E}_{T,d} := \left(\sum_{n=1}^{N_d} \omega_n^d \left| \mathcal{R}_{d,\theta_m^*}(x_n, t_n) \right|^2 \right)^{1/2}.$$

- The interior PDE training errors

$$\mathcal{E}_{T,int} := \left(\sum_{n=1}^{N_{int}} \omega_n^{int} \left| \mathcal{R}_{int,\theta_f^*,\theta_m^*,\theta_e^*}(\tilde{x}_n, \tilde{t}_n) \right|^2 \right)^{1/2}.$$

- The initial condition training errors $\mathcal{E}_{T,tb,0} := \mathcal{E}_{T,tb} + \mathcal{E}_{T,tb,1}$, where

$$\begin{cases} \mathcal{E}_{T,tb,0} := \left(\sum_{n=1}^{N_{tb}} \omega_n^{tb,0} \left| \mathcal{R}_{tb,\theta_m^*}(\bar{x}_n) \right|^2 \right)^{1/2}, \\ \mathcal{E}_{T,tb,1} := \left(\sum_{n=1}^{N_{tb}} \omega_n^{tb,1} \left| \partial_t \mathcal{R}_{tb,\theta_m^*}(\bar{x}_n) \right|^2 \right)^{1/2}. \end{cases}$$

- The spatial boundary condition training errors $\mathcal{E}_{T,sb} := \mathcal{E}_{T,sb,0} + \mathcal{E}_{T,sb,1} + \mathcal{E}_{T,sb,2} + \mathcal{E}_{T,sb,3}$, where

$$\begin{cases} \mathcal{E}_{T,sb,0} := \left(\sum_{n=1}^{N_{sb}} \omega_n^{sb,0} \left| \mathcal{R}_{sb,\theta_m^*}(\hat{x}_n, \hat{t}_n) \right|^2 \right)^{1/2}, \\ \mathcal{E}_{T,sb,1} := \left(\sum_{n=1}^{N_{sb}} \omega_n^{sb,1} \left| \frac{\partial \mathcal{R}_{sb,\theta_m^*}}{\partial \bar{\mathbf{n}}}(\hat{x}_n, \hat{t}_n) \right|^2 \right)^{1/2}, \\ \mathcal{E}_{T,sb,2} := \left(\sum_{n=1}^{N_{sb}} \omega_n^{sb,2} \left| \frac{\partial \mathcal{R}_{sb,\theta_m^*}}{\partial t}(\hat{x}_n, \hat{t}_n) \right|^2 \right)^{1/2}, \\ \mathcal{E}_{T,sb,3} := \left(\sum_{n=1}^{N_{sb}} \omega_n^{sb,3} \left| \frac{\partial^2 \mathcal{R}_{sb,\theta_m^*}}{\partial t \partial \bar{\mathbf{n}}}(\hat{x}_n, \hat{t}_n) \right|^2 \right)^{1/2}. \end{cases}$$

We can compute these errors from the loss function (4.3) using automatic differentiation in case of derivative terms.

The above derivations have established the following generalization error estimates for the inverse problem.

Theorem 3. Under the assumption of Theorem 1, there exists a unique solution to the inverse problem (1.6). Moreover, for the approximate solution u_e^* of the forward problem with θ_e^* being a global minimizer of the loss function $J_1^N(\theta_e)$, and (μ_f^*, u_m^*) of the inverse problem with (θ_f^*, θ_m^*) being a global minimizer of the loss function $J_2^N(\theta_f, \theta_m)$, we have the following generalization error estimates

$$\begin{aligned}\mathcal{E}_{G, u_e} &\leq C \left(\bar{\mathcal{E}}_{T, int} + \bar{\mathcal{E}}_{T, sb} + \bar{\mathcal{E}}_{T, tb} + \bar{C}_q^{\frac{1}{2}} \bar{N}^{\frac{-\bar{\alpha}}{2}} \right), \\ \mathcal{E}_{G, \bar{p}} &\leq C \left(\bar{\mathcal{E}}_{T, int} + \bar{\mathcal{E}}_{T, sb} + \bar{\mathcal{E}}_{T, tb} + \mathcal{E}_{T, d} + \mathcal{E}_{T, int} + \mathcal{E}_{T, sb} + \mathcal{E}_{T, tb} + C_q^{\frac{1}{2}} N^{\frac{-\alpha}{2}} + \delta \right),\end{aligned}\quad (4.9)$$

where the constants C depend only on Ω and T . Furthermore, these constants are selected as

$$\begin{aligned}\bar{C}_q^{\frac{1}{2}} \bar{N}^{\frac{-\bar{\alpha}}{2}} &= \max \left\{ \bar{C}_q^{\frac{1}{2}} N_{int}^{\frac{-\bar{\alpha}_{int}}{2}}, \bar{C}_{qt}^{\frac{1}{2}} N_{tb}^{\frac{-\bar{\alpha}_{tb}}{2}}, \bar{C}_{qs}^{\frac{1}{2}} N_{sb}^{\frac{-\bar{\alpha}_{sb}}{2}} \right\}, \\ C_q^{\frac{1}{2}} N^{\frac{-\alpha}{2}} &= \max_{k=0,1, j=0,1,2,3} \left\{ \bar{C}_q^{\frac{1}{2}} \bar{N}^{\frac{-\bar{\alpha}}{2}}, C_{qd}^{\frac{1}{2}} N_d^{\frac{-\alpha_d}{2}}, C_q^{\frac{1}{2}} N_{int}^{\frac{-\alpha_{int}}{2}}, C_{qt,k}^{\frac{1}{2}} N_{tb}^{\frac{-\alpha_{tb,k}}{2}}, C_{qs,j}^{\frac{1}{2}} N_{sb}^{\frac{-\alpha_{sb,j}}{2}} \right\},\end{aligned}$$

with the constant

$$\bar{C}_q = \bar{C}_q \left(\left\| \mathcal{R}_{int, \theta_e^*} \right\|_{C(\Omega_T)} \right), \quad \bar{C}_{qs} = \bar{C}_{qs} \left(\left\| \mathcal{R}_{sb, \theta_e^*} \right\|_{C(\partial\Omega_T)} \right), \quad \bar{C}_{qt} = \bar{C}_{qt} \left(\left\| \mathcal{R}_{tb, \theta_e^*} \right\|_{C(\Omega)} \right),$$

and

$$\begin{aligned}C_{qd} &= C_{qd} \left(\left\| q^* \mathcal{R}_{d, \theta_m^*} \right\|_{C(\Omega)} \right), & C_q &= C_q \left(\left\| \mathcal{R}_{int, \theta_e^*, \theta_f^*, \theta_m^*} \right\|_{C(\Omega_T)} \right), \\ C_{qs,0} &= C_{qs,0} \left(\left\| \mathcal{R}_{sb, \theta_m^*} \right\|_{C(\partial\Omega_T)} \right), & C_{qs,1} &= C_{qs,1} \left(\left\| \frac{\partial \mathcal{R}_{sb, \theta_m^*}}{\partial \vec{\mathbf{n}}} \right\|_{C(\partial\Omega_T)} \right), \\ C_{qs,2} &= C_{qs,2} \left(\left\| \frac{\partial \mathcal{R}_{sb, \theta_m^*}}{\partial t} \right\|_{C(\partial\Omega_T)} \right), & C_{qs,3} &= C_{qs,3} \left(\left\| \frac{\partial^2 \mathcal{R}_{sb, \theta_m^*}}{\partial t \partial \vec{\mathbf{n}}} \right\|_{C(\partial\Omega_T)} \right), \\ C_{qt,0} &= C_{qt,0} \left(\left\| \mathcal{R}_{tb, \theta_m^*} \right\|_{C(\Omega)} \right), & C_{qt,1} &= C_{qt,1} \left(\left\| \frac{\partial \mathcal{R}_{tb, \theta_m^*}}{\partial t} \right\|_{C(\Omega)} \right),\end{aligned}$$

where we denote $\Omega_T := \Omega \times (0, T)$ and $\partial\Omega_T := \partial\Omega \times (0, T)$.

Proof. First, we will derive the estimates on the first formulation of (4.8). Introduce $\hat{u}_e := u_e^* - u_{e,ex}$, where $u_e^* = u_{e, \theta_e^*}$ and $\hat{u}_e(x, t)$ satisfies

$$\begin{cases} (c^{-1} \partial_t + \mathcal{A}) \hat{u}_e(x, t) = \mathcal{R}_{int, \theta_e^*}, & (x, t) \in \Omega \times (0, T), \\ \hat{u}_e(x, 0) = \mathcal{R}_{tb, \theta_e^*}(x), & x \in \Omega, \\ \mathcal{B} \hat{u}_e(x, t) = \mathcal{R}_{sb, \theta_e^*}(x, t), & (x, t) \in \partial\Omega \times (0, T). \end{cases}$$

Using the regularity estimates in [12], there holds

$$\begin{aligned}\|\hat{u}_e\|_{L^\infty(0,T;L^2(\Omega))} &= \|u_e^* - u_{e,ex}\|_{L^\infty(0,T;L^2(\Omega))} \\ &\leq C \|\mathcal{R}_{int, \theta_e^*}\|_{L^2(0,T;L^2(\Omega))} + \|\mathcal{R}_{tb, \theta_e^*}\|_{L^2(\Omega)} + \|\mathcal{R}_{sb, \theta_e^*}\|_{L^2(0,T;H^{-3/2}(\partial\Omega))}.\end{aligned}\quad (4.10)$$

Then, we will derive the estimates on the second formulation of (4.8). Introducing $\hat{u}_m := u_m^* - u_{m,ex}$ with

$$u_m^* = u_{m, \theta_m^*} = u_{m, \theta_m^*} [\mu_f, \theta_f^*, u_{e, \theta_e^*}] = u_m^* [\mu_f^*, u_e^*],$$

we have the equation

$$\begin{cases} (c^{-1}\partial_t + \mathcal{A}) \hat{u}_m(x, t) = \mu_f^* u_e^* - \mu_{f,ex} u_{e,ex} + \mathcal{R}_{int, \theta_m^*, \theta_f^*, \theta_e^*}, & (x, t) \in \Omega \times (0, T), \\ \hat{u}_m(x, 0) = \mathcal{R}_{tb, \theta_m^*}(x), & x \in \Omega, \\ \mathcal{B}\hat{u}_m(x, t) = \mathcal{R}_{sb, \theta_m^*}(x, t), & (x, t) \in \partial\Omega \times (0, T), \end{cases}$$

and the observation data

$$\frac{\partial \hat{u}_m}{\partial \vec{\mathbf{n}}} = \frac{\partial u_{m, \theta_m^*}}{\partial \vec{\mathbf{n}}} - \frac{\partial u_{m, ex}}{\partial \vec{\mathbf{n}}} = \mathcal{R}_{d, \theta_m^*}(x, t) + \varphi^\delta - \varphi, \quad (x, t) \in \Gamma \times (0, T].$$

We make the decomposition $\hat{u}_m := \hat{u}_{m,1} + \hat{u}_{m,2}$, where $\hat{u}_{m,1}, \hat{u}_{m,2}$ satisfy

$$\begin{cases} (c^{-1}\partial_t + \mathcal{A}) \hat{u}_{m,1}(x, t) = \mu_f^* u_e^* - \mu_{f,ex} u_{e,ex}, & (x, t) \in \Omega \times (0, T), \\ \hat{u}_{m,1}(x, 0) = 0, & x \in \Omega, \\ \mathcal{B}\hat{u}_{m,1}(x, t) = 0, & (x, t) \in \partial\Omega \times (0, T), \end{cases}$$

with

$$\frac{\partial \hat{u}_{m,1}}{\partial \vec{\mathbf{n}}} = \frac{\partial \hat{u}_m}{\partial \vec{\mathbf{n}}} - \frac{\partial \hat{u}_{m,2}}{\partial \vec{\mathbf{n}}} = \mathcal{R}_{d, \theta_m^*}(x, t) + (\varphi^\delta - \varphi) - \frac{\partial \hat{u}_{m,2}}{\partial \vec{\mathbf{n}}}, \quad (x, t) \in \Gamma \times (0, T],$$

and

$$\begin{cases} (c^{-1}\partial_t + \mathcal{A}) \hat{u}_{m,2}(x, t) = \mathcal{R}_{int, \theta_m^*, \theta_f^*, \theta_e^*}, & (x, t) \in \Omega \times (0, T), \\ \hat{u}_{m,2}(x, 0) = \mathcal{R}_{tb, \theta_m^*}(x), & x \in \Omega, \\ \mathcal{B}\hat{u}_{m,2}(x, t) = \mathcal{R}_{sb, \theta_m^*}(x, t), & (x, t) \in \partial\Omega \times (0, T), \end{cases}$$

respectively.

Next we split $\hat{u}_{m,1} = \hat{u}_{m,11} + \hat{u}_{m,12}$, where $\hat{u}_{m,11}, \hat{u}_{m,12}$ satisfy

$$\begin{cases} (c^{-1}\partial_t + \mathcal{A}) \hat{u}_{m,11}(x, t) = (\mu_f^* - \mu_{f,ex}) u_{e,ex}, & (x, t) \in \Omega \times (0, T), \\ \hat{u}_{m,11}(x, 0) = 0, & x \in \Omega, \\ \mathcal{B}\hat{u}_{m,11}(x, t) = 0, & (x, t) \in \partial\Omega \times (0, T), \end{cases} \quad (4.11)$$

with

$$\begin{aligned} \frac{\partial \hat{u}_{m,11}}{\partial \vec{\mathbf{n}}} &= \frac{\partial \hat{u}_{m,1}}{\partial \vec{\mathbf{n}}} - \frac{\partial \hat{u}_{m,12}}{\partial \vec{\mathbf{n}}} \\ &= \mathcal{R}_{d, \theta_m^*}(x, t) + (\varphi^\delta - \varphi) - \frac{\partial \hat{u}_{m,2}}{\partial \vec{\mathbf{n}}} - \frac{\partial \hat{u}_{m,12}}{\partial \vec{\mathbf{n}}}, \quad (x, t) \in \Gamma \times (0, T], \end{aligned} \quad (4.12)$$

and

$$\begin{cases} (c^{-1}\partial_t + \mathcal{A}) \hat{u}_{m,12}(x, t) = \mu_f^*(u_e^* - u_{e,ex}), & (x, t) \in \Omega \times (0, T), \\ \hat{u}_{m,12}(x, 0) = 0, & x \in \Omega, \\ \mathcal{B}\hat{u}_{m,12}(x, t) = 0, & (x, t) \in \partial\Omega \times (0, T). \end{cases}$$

For the inverse problem (4.11)-(4.12), according to conditional stability result, i.e, Theorem 2, we get

$$\|\vec{p}_* - \vec{p}_{ex}\|_{\mathcal{L}} \leq C \left\| \frac{\partial \hat{u}_{m,11}}{\partial \vec{\mathbf{n}}} \right\|_{L^2(\Gamma \times (0, T))}$$

$$\begin{aligned}
&= C \left\| \mathcal{R}_{d,\theta_m^*}(x,t) + (\varphi^\delta - \varphi) - \frac{\partial \hat{u}_{m,2}}{\partial \vec{\mathbf{n}}} - \frac{\partial \hat{u}_{m,12}}{\partial \vec{\mathbf{n}}} \right\|_{L^2(\Gamma \times (0,T))} \\
&\leq \|\mathcal{R}_{d,\theta_m^*}\|_{L^2(\Gamma \times (0,T))} + \|\varphi^\delta - \varphi\|_{L^2(\Gamma \times (0,T))} + \left\| \frac{\partial \hat{u}_{m,2}}{\partial \vec{\mathbf{n}}} \right\|_{L^2(\Gamma \times (0,T))} + \left\| \frac{\partial \hat{u}_{m,12}}{\partial \vec{\mathbf{n}}} \right\|_{L^2(\Gamma \times (0,T))} \\
&\leq \|\mathcal{R}_{d,\theta_m^*}\|_{L^2(\Gamma \times (0,T))} + \left\| \frac{\partial \hat{u}_{m,2}}{\partial \vec{\mathbf{n}}} \right\|_{L^2(\partial\Omega \times (0,T))} + \left\| \frac{\partial \hat{u}_{m,12}}{\partial \vec{\mathbf{n}}} \right\|_{L^2(\partial\Omega \times (0,T))} + \delta.
\end{aligned} \tag{4.13}$$

Using trace theorem and Sobolev embedding theorem, we further get

$$\begin{aligned}
\|\vec{p}_* - \vec{p}_{ex}\|_{\mathcal{L}} &\leq \|\mathcal{R}_{d,\theta_m^*}\|_{L^2(\Gamma \times (0,T))} + \|\hat{u}_{m,2}\|_{L^2(0,T;H^{3/2}(\Omega))} + \|\hat{u}_{m,12}\|_{L^2(0,T;H^{3/2}(\Omega))} + \delta \\
&\leq \|\mathcal{R}_{d,\theta_m^*}\|_{L^2(\Gamma \times (0,T))} + \|\hat{u}_{m,2}\|_{L^2(0,T;H^2(\Omega))} + \|\hat{u}_{m,12}\|_{L^2(0,T;H^2(\Omega))} + \delta.
\end{aligned} \tag{4.14}$$

According to the estimates in [12], the second term of the inequality (4.14) satisfies

$$\begin{aligned}
\|\hat{u}_{m,2}\|_{L^2(0,T;H^2(\Omega))} &\leq C \left(\|\mathcal{R}_{int,\theta_m^*,\theta_f^*,\theta_e^*}\|_{L^2(0,T;L^2(\Omega))} + \|\mathcal{R}_{tb,\theta_m^*}\|_{H_0^1(\Omega)} \right. \\
&\quad \left. + \|\mathcal{R}_{sb,\theta_m^*}\|_{L^2(0,T;H^{1/2}(\partial\Omega))} + \|\partial_t \mathcal{R}_{sb,\theta_m^*}\|_{L^2(0,T;H^{1/2}(\partial\Omega))} \right) \\
&\leq C \left(\|\mathcal{R}_{int,\theta_m^*,\theta_f^*,\theta_e^*}\|_{L^2(0,T;L^2(\Omega))} + \|\mathcal{R}_{tb,\theta_m^*}\|_{H_0^1(\Omega)} + \|\mathcal{R}_{sb,\theta_m^*}\|_{H^1(0,T;H^1(\partial\Omega))} \right).
\end{aligned} \tag{4.15}$$

Using (4.10), the third term in (4.14) satisfies

$$\begin{aligned}
\|\hat{u}_{m,12}\|_{L^2(0,T;H^2(\Omega))} &\leq C \|\mu_f^*(u_e^* - u_{e,ex})\|_{L^2(0,T;L^2(\Omega))} \\
&\leq C \|(u_e^* - u_{e,ex})\|_{L^\infty(0,T;L^2(\Omega))} \\
&\leq C \left(\|\mathcal{R}_{int,\theta_e^*}\|_{L^2(0,T;L^2(\Omega))} + \|\mathcal{R}_{tb,\theta_e^*}\|_{L^2(\Omega)} + \|\mathcal{R}_{sb,\theta_e^*}\|_{L^2(0,T;H^{-3/2}(\partial\Omega))} \right) \\
&\leq C \left(\|\mathcal{R}_{int,\theta_e^*}\|_{L^2(0,T;L^2(\Omega))} + \|\mathcal{R}_{tb,\theta_e^*}\|_{L^2(\Omega)} + \|\mathcal{R}_{sb,\theta_e^*}\|_{L^2(0,T;L^2(\partial\Omega))} \right).
\end{aligned} \tag{4.16}$$

Combining (4.13)-(4.16) together and using the Sobolev embedding theorem, we get the generalization error estimate for \vec{p}

$$\begin{aligned}
\|\vec{p}_* - \vec{p}_{ex}\|_{\mathcal{L}} &\leq C \left(\|\mathcal{R}_{int,\theta_e^*}\|_{L^2(0,T;L^2(\Omega))} + \|\mathcal{R}_{tb,\theta_e^*}\|_{L^2(\Omega)} + \|\mathcal{R}_{sb,\theta_e^*}\|_{L^2(0,T;L^2(\partial\Omega))} + \delta \right. \\
&\quad \left. + \|\mathcal{R}_{d,\theta_m^*}\|_{L^2(\Gamma \times (0,T))} + \|\mathcal{R}_{int,\theta_m^*,\theta_f^*,\theta_e^*}\|_{L^2(0,T;L^2(\Omega))} + \|\mathcal{R}_{tb,\theta_m^*}\|_{H_0^1(\Omega)} \right. \\
&\quad \left. + \|\mathcal{R}_{sb,\theta_m^*}\|_{H^1(0,T;H^1(\partial\Omega))} \right).
\end{aligned} \tag{4.17}$$

The formulations in (4.9) are generated by applying (4.10) and (4.17), with the quadrature rules (2.5) respectively. The proof is complete. \square

The above estimates include the difference between the underlying solution and the approximation solution produced by data-driven method of the inverse problem, which represent the approximation of the problem in a finite dimensional space, and essentially reflect the stability due to both the model itself and the reconstruction scheme. Therefore, based on the result of Theorem 3, we can conduct the reconstruction algorithms both for excitation process to solve the direct problem and emission process to solve the inverse problem.

Remark 4.3. In this work, the attempt to evaluate the generalization error estimate for unknown u_m employing the generalization error (4.17) is frustrated. This is because the norm equality between $\|\vec{p}\|_{\mathcal{L}}$ and $\|L\vec{p}\|_{L^2(0,T;L^2(\Omega))}$ is not proven. In the future, we will explore the suitable norm on \vec{p} and give the generalization error estimate for u_m .

5 Numerical inversions.

For actual implementation, we firstly parameterize u_e by deep neural networks u_{e,θ_e} with network parameters θ_e . Minimizing the loss function (4.1) to search for the optimal parameters θ_e^* . Then, for the obtained $u_e^* := u_{e,\theta_e^*}$, we will consider to recover the solution (μ_f, u_m) for inverse problems. We also parameterize μ_f and u_m by deep neural networks μ_{f,θ_f} and u_{m,θ_m} with network parameters θ_f and θ_m , respectively. Minimizing the loss function (4.2) to search for the optimal parameters θ_f^* and θ_m^* , the corresponding $\mu_f^* = \mu_{f,\theta_f^*}$ and $u_m^* = u_{m,\theta_m^*}$ are the approximate solution of the inverse problem. We construct the next Algorithms 1 and 2 to solve the direct problem (1.1) and the inverse problem (1.6) respectively.

Algorithm 1: Data-driven solution of the direct problem (1.1).

Require: Boundary input $g(x, t)$ for the excitation process (1.1).

Initialize Network architectures u_{e,θ_e} and parameters θ_e .

for $j = 1, \dots, K_1$ **do**

 Sample $\mathcal{S}_{int}, \mathcal{S}_{sb}, \mathcal{S}_{tb}$.

$\theta_e \leftarrow \text{Adam}(-\nabla_{\theta_e} J_1^N(\theta_e), \tau_{\theta_e})$,

end for

Ensure: u_{e,θ_e^*} .

Algorithm 2: Data-driven solution of the inverse problem (1.6).

Require: The obtained u_{e,θ_e^*} and noisy measurement data φ^δ for the inverse problem.

Initialize Network architectures $(\mu_{f,\theta_f}, u_{m,\theta_m})$ and parameters (θ_f, θ_m) .

for $j = 1, \dots, K_2$ **do**

 Sample $\mathcal{S}_d, \mathcal{S}_{int}, \mathcal{S}_{sb}, \mathcal{S}_{tb}$.

$\theta_f \leftarrow \text{Adam}(-\nabla_{\theta_f} J_2^N(\theta_f, \theta_m), \tau_{\theta_f}, \lambda)$,

$\theta_m \leftarrow \text{Adam}(-\nabla_{\theta_m} J_2^N(\theta_f, \theta_m), \tau_{\theta_m}, \lambda)$,

end for

Ensure: $(\mu_{f,\theta_f^*}, u_{m,\theta_m^*})$.

The above minimization problems are to search the minimizer of the possibly non-convex function $J_1^N(\theta_e)$ and $J_2^N(\theta_f, \theta_m)$ over $\Theta \subset \mathbb{R}^{\mathcal{M}}$ for possibly very large \mathcal{M} . The hyper-parameters $(\tau_{\theta_e}, \tau_{\theta_f}, \tau_{\theta_m})$ are learning rates and λ are balance hyper-parameters between PDE and measurement data residuals. The optimizer is Adam (Adaptive Moment Estimation), which is an optimization algorithm commonly used in deep learning for training neural networks. The robust analysis for hyper-parameters λ will be studied in the numerical implementation subsection.

Example 1: The boundary input of excitation process is set as

$$\mathcal{B}u_e = -20tx(x-1), \quad (x, y, t) \in \partial\Omega \times (0, T),$$

where the diffusion domain is $\Omega = (0, 1)^2$, the final time is $T = 1$ and the exact source μ_f of emission system is given as

$$\mu_f(x, y, t) = 5 + t + \cos(\pi x) \cos(\pi y),$$

which is smooth on the whole time and space domain $\Omega \times (0, T)$. The exact measurement will be

$$\varphi(x, y, t) = \frac{\partial u_m}{\partial \mathbf{n}} \Big|_{\Gamma \times (0, T)},$$

with $\Gamma \subset \partial\Omega$, and in our experiments the noisy data is set as

$$\varphi^\delta(x, y, t) := \varphi(x, y, t) + \delta \cdot (2 \text{rand}(\text{shape}(\varphi(x, y, t))) - 1), \quad (5.1)$$

where $\text{rand}(\text{shape}(\varphi))$ is a random variable generated by uniform distribution in $[0, 1]$.

For the implementation details, we use a fully connected neural network for u_{e, θ_e} with 3 hidden layers, each layer with a width of 20. We take $N = N_{int} + N_{sb} + N_{tb} = 256 + 256 \times 4 + 256 = 1536$ as the number of collocation points, which are randomly sampled in three different domains, i.e., interior spatio-temporal domain, spatial and temporal boundary domain. The collocation points are selected with respect to uniform distributions. The activation function is \tanh . The number of training epochs is set to be 5×10^4 , and the initial learning rates start with 0.001 and shrink 10 times every 2×10^4 iteration. For the inversion of emission process, we also use the fully connected neural network both for μ_{f, θ_f} and u_{m, θ_m} with 3 hidden layers, each layer with a width of 20. The number of training points is $N = N_{int} + N_{sb} + N_{tb} + N_d = 500 + 500 \times 4 + 500 + 500 = 3500$, which are randomly sampled in four different domains, i.e., interior spatio-temporal domain, spatial and temporal boundary domain, and measurement domain. The collocation points are selected with respect to uniform distributions. The activation functions for μ_{f, θ_f} and u_{m, θ_m} are both \tanh , and the hyper-parameter is $\lambda = 100$. The number of training epochs is set to be 2×10^4 , and the initial learning rates start with 0.001 and shrink 10 times every 2000 iteration. The test sets are chosen by a uniform mesh

$$\mathcal{T} := \{(t_k, x_i, y_j) : k, i, j = 0, 1, \dots, 49\} \subset \Omega_T. \quad (5.2)$$

Figure 1 shows the exact (upper line), the reconstruction results (middle line) for absorption coefficient μ_f and the corresponding absolute pointwise error (bottom line) at different times $t = 0, 2/7, 4/7, 1$, respectively, with the noisy level $\delta = 0.01$. We can find that the reconstruction results for μ_f is well even with high noise of measurement data. Figure 2 shows the reconstruction results (upper line) and the corresponding absolute pointwise error (bottom line) for μ_f at fixed time $t = 1$ with different noisy level $\delta = 0, 0.01, 0.05, 0.1$, respectively. Meanwhile, the numerical solution for excitation process u_e (upper line) are shown in Figure 3, which also presents the reconstruction of emission solution u_m at different times $t = 2/7, t = 3/7, t = 5/7$ and $t = 1$, respectively, with various noisy levels $\delta = 0$ (second line), $\delta = 0.01$ (third line) and $\delta = 0.1$ (bottom line). We can see the evolution of the excitation solution for u_e over time, and the reconstruction accuracy for u_m deteriorates as the noise level increasing, but the performance is still satisfactory.

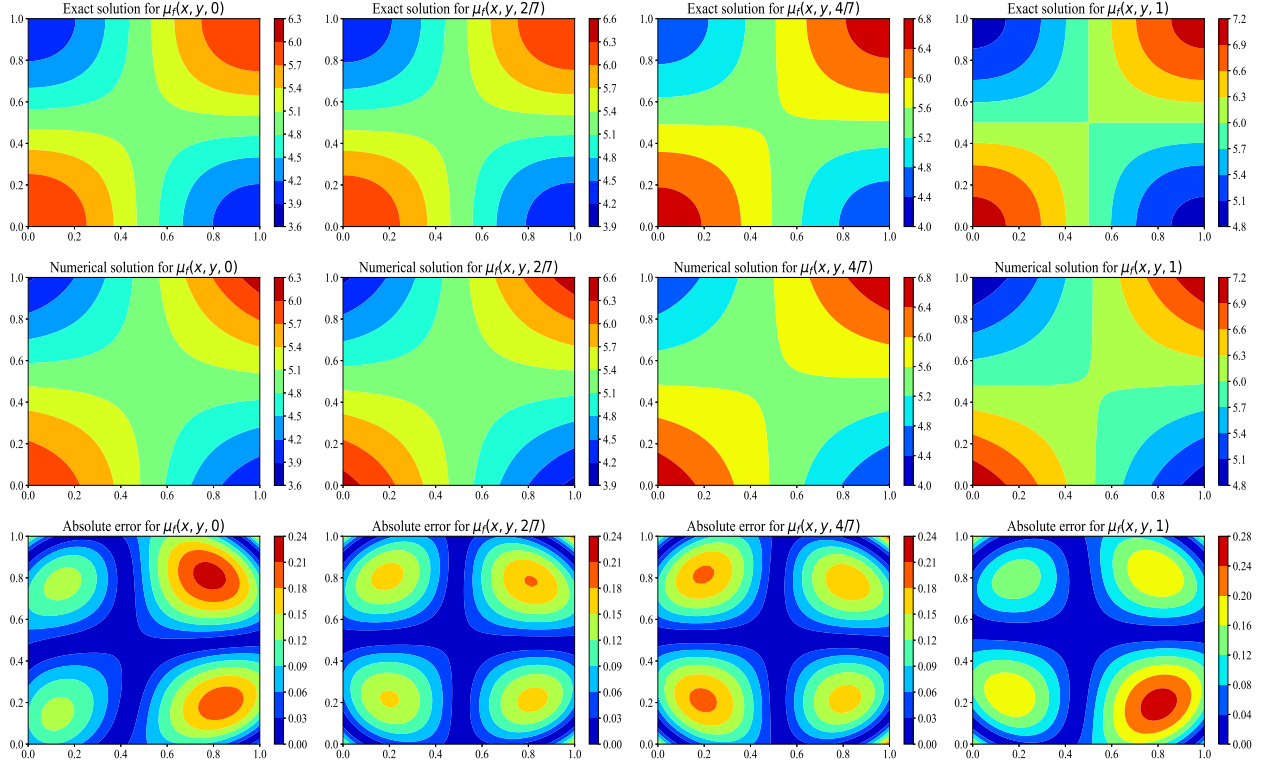


Figure 1: The exact (upper), reconstruction results (middle) and corresponding absolute pointwise errors (bottom) for absorption coefficient μ_f at different times with noisy level $\delta = 0.01$.

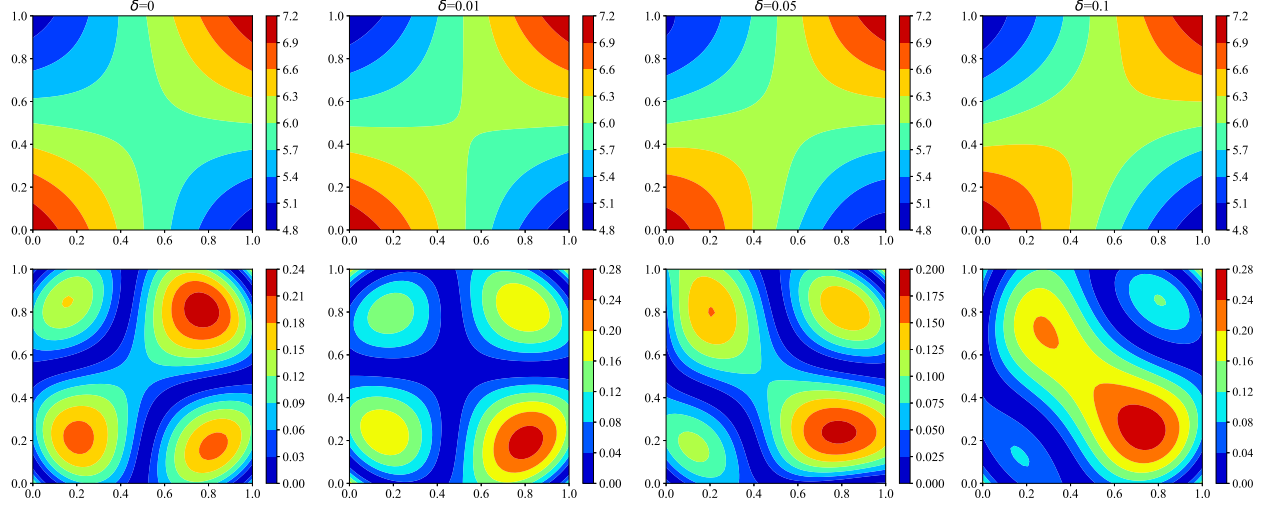


Figure 2: The reconstruction results (upper line) and corresponding absolute pointwise errors (bottom line) for absorption coefficient $\mu_f(x, y, 1)$ with different noisy levels $\delta = 0, 0.01, 0.05, 0.1$.

Example 2: The boundary input of excitation process is set as

$$\mathcal{B}u_e = -20tx(x-1), \quad (x, y, t) \in \partial\Omega \times [0, T],$$

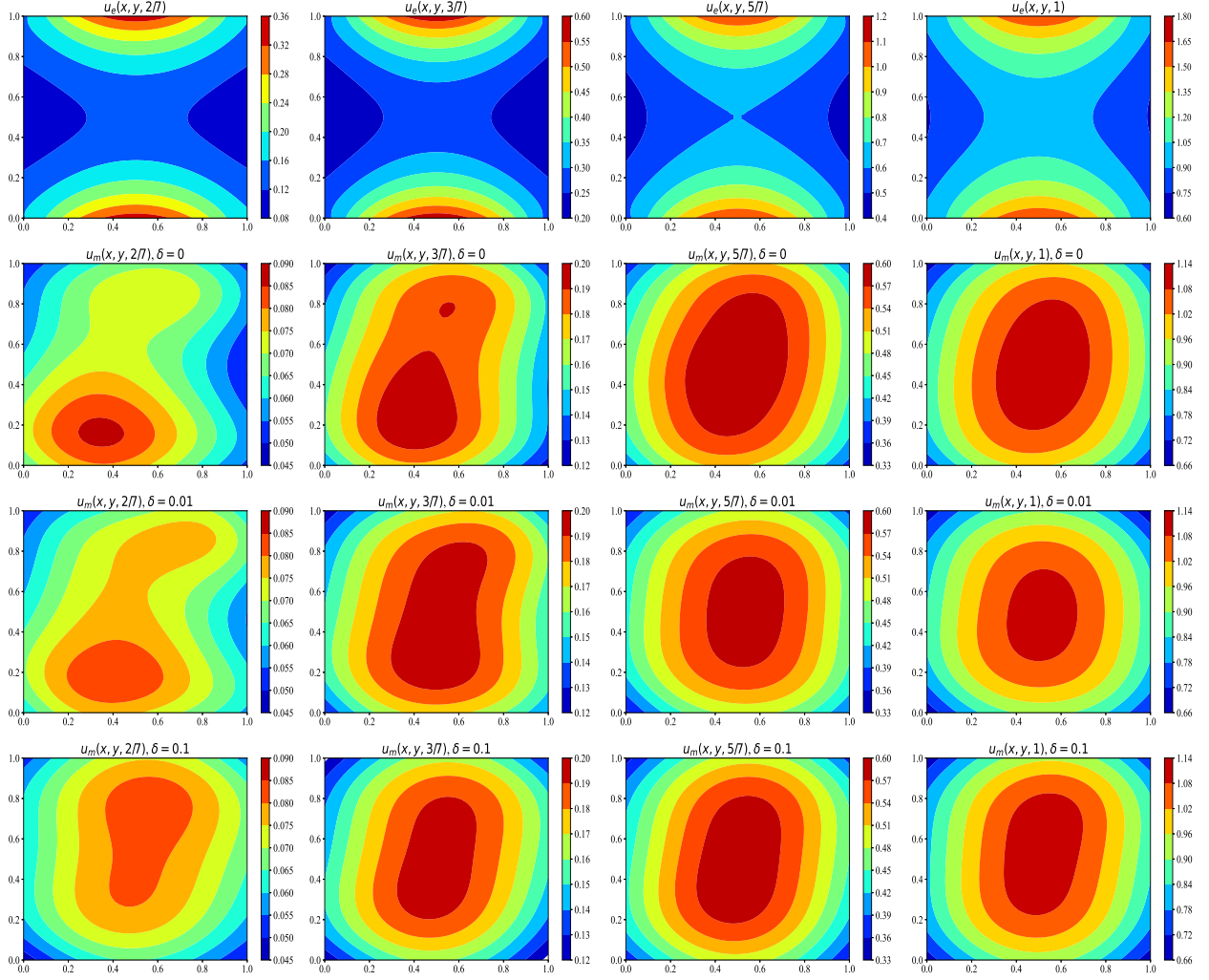


Figure 3: The numerical results for u_e and u_m at different times $t = 2/7, 3/7, 5/7, 1$ with various noisy levels $\delta = 0, 0.01, 0.1$.

where the diffusion domain is $\Omega = (0, 1)^2$, the final time is $T = 1$ and the exact source μ_f of emission system is given as

$$\mu_f(x, y, t) = (t + 1)f(r)$$

with

$$f(r) = \begin{cases} 15(\cos r - \sqrt{3}/2) + 2, & 0 \leq r \leq \pi/6, \\ 2, & \text{otherwise}, \end{cases}$$

$$r(x, y) = \sqrt{(x - 0.5)^2 + (y - 0.5)^2},$$

which is continuous but not smooth in spatial domain. The noisy measurement data is generated by the same way in (5.1).

For the implementation details of excitation process, the architectures of the neural networks, the training points sampling and the test sets are the same as Example 1 to get u_{e,θ_e} . For the inversion of emission process, we also use the fully connected neural network both for

μ_{f,θ_f} and u_{m,θ_m} with 3 hidden layers, each layer with a width of 20. The number of training points is $N = N_{int} + N_{sb} + N_{tb} + N_d = 500 + 500 \times 4 + 500 + 500 = 3500$, which are randomly sampled in four different domains, i.e., interior spatio-temporal domain, spatial and temporal boundary domain, and measurement domain. The collocation points are selected with respect to uniform distributions. The activation functions for μ_{f,θ_f} and u_{m,θ_m} are both \tanh , and the hyper-parameter is $\lambda = 100$. The number of training epochs is set to be 4×10^4 , and the initial learning rates start with 0.002 and shrink 10 times every 2×10^4 iteration. The test sets are chosen by a uniform mesh (5.2).

Since the noisy level of the measurement data affects the reconstruction accuracy, in this simulation, we test the training performance for various noisy levels. Figure 4 records the training process, i.e., the training loss, the relative error for the reconstruction of μ_f with respect to the iterations for different noise levels $\delta = 0, 0.1\%, 1\%, 10\%$ by the proposed scheme.

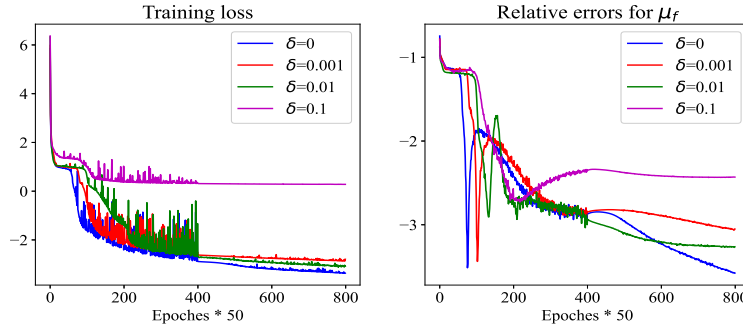


Figure 4: The training loss (left) and the relative error for μ_f (right) after logarithmic re-scaling.

The distribution of the absorption coefficient $\mu_f(x, t)$ also depends on the time t , Figure 5 shows the time-series relative error of the recovered μ_f with various noise levels. As shown in this figure, the training performance deteriorates as the noise level of the measurement data increasing.

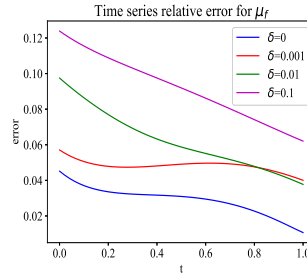


Figure 5: The time series relative error (test) for μ_f after logarithmic re-scaling for different noisy data.

Figure 6 shows the exact absorption coefficient at final time $t = 1$. Figure 7 shows the reconstruction results for μ_f at final time $t = 1$ by optimizing the proposed loss function (upper line) and the corresponding absolute pointwise error (bottom line) for various noisy levels $\delta = 0, 0.1\%, 1\%, 10\%$. Meanwhile, the numerical solution u_e at different times for excitation process are shown in Figure 8. Figure 9 presents the reconstruction of emission solution u_m at different times $t = 2/7, t = 3/7$ and $t = 1$, respectively, with various noisy

levels. We can see that the reconstruction accuracy deteriorates as the noise level of the measurement data increasing, but the performance is still satisfactory.

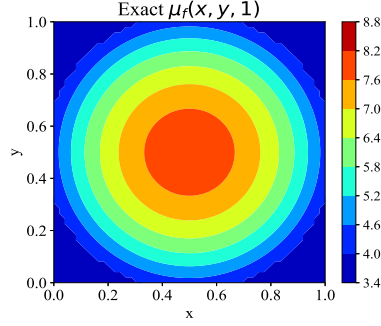


Figure 6: The exact absorption coefficient μ_f at final time $t = 1$.

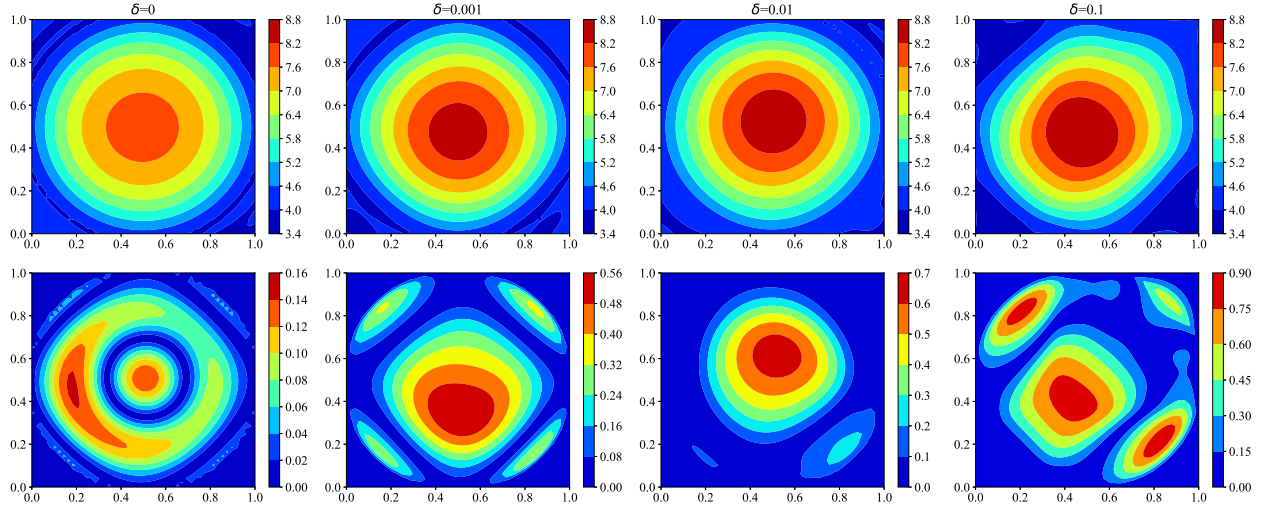


Figure 7: The reconstruction of absorption coefficient μ_f (upper line) and corresponding absolute point-wise error $|\mu_f - \mu_f^*|$ (bottom line) for various noisy level measurement data at final time $t = 1$.

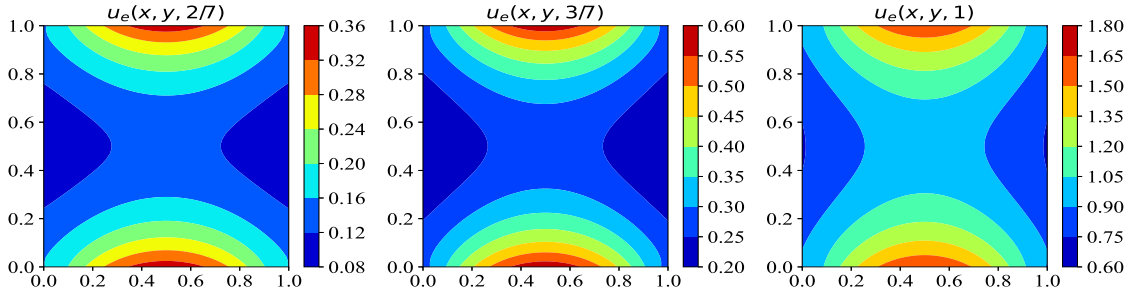


Figure 8: The numerical solution u_e for excitation process at different times $t = 2/7$ (left), $t = 3/7$ (middle) and at final time $t = 1$ (right), respectively.

In order to evaluate the effectiveness of the proposed scheme in terms of hyper-parameters, some experiments are conducted. Specifically, we examine the impact of the balance hyper-parameter λ in (4.2). For the fixed hidden layers ($NL = 3$) and fixed neurons per-layer

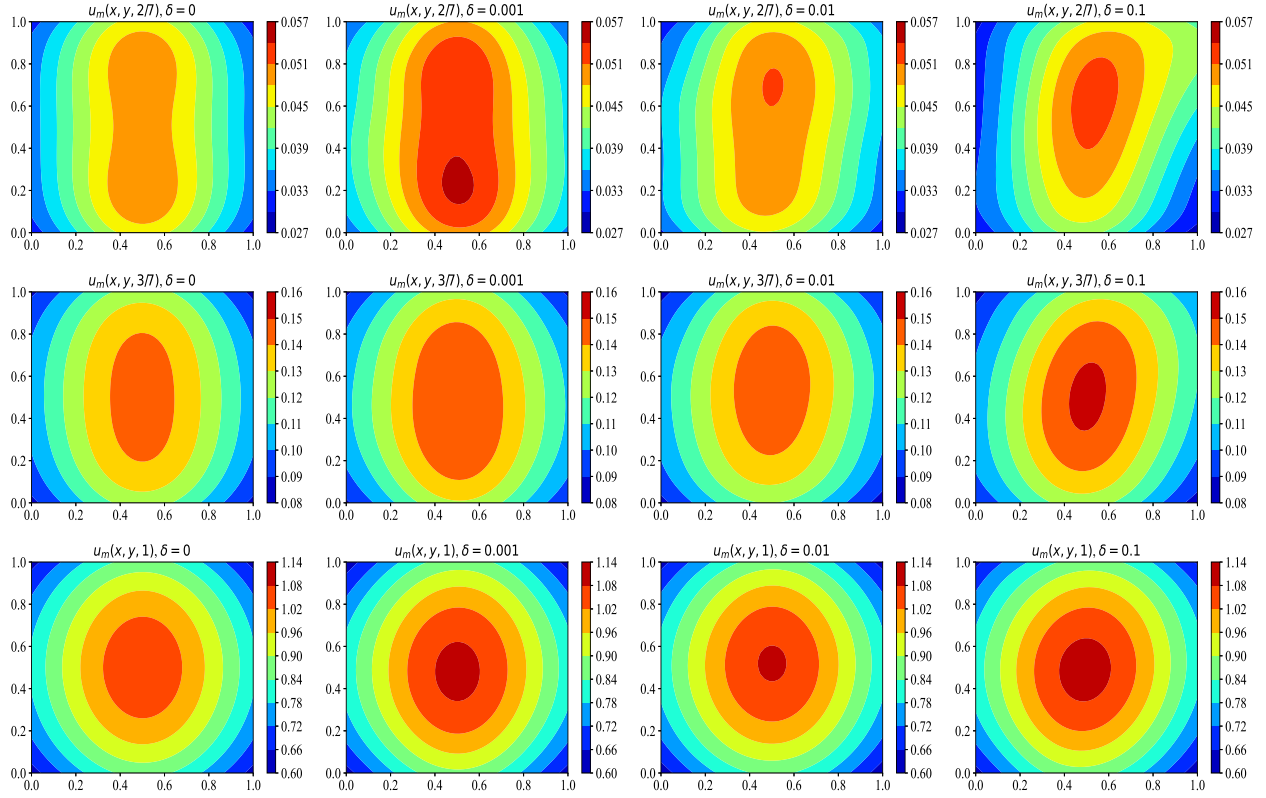


Figure 9: The reconstruction of the emission solution u_m at different times $t = 2/7$ (upper line), $t = 3/7$ (middle line) and at final time $t = 1$ (bottom line), respectively, with various noisy levels $\delta = 0, 0.1\%, 1\%, 10\%$.

($NN = 20$), we compute the reconstruction errors (mean and standard deviation) for μ_f and u_m with different values of λ , such as 10000, 1000, 100, 10, 1, 0.1. The results of these experiments are presented in Table 1, which indicate that the performance of the inverse problem is highly dependent on the balance hyper-parameter λ . Specifically, we find that the relative reconstruction errors are optimized when λ is between 10 to 1000. Furthermore, we observe that the reconstruction errors increase significantly as λ exceeds this optimal value. These results suggest that the selection of the balance hyper-parameter is critical to achieving good performance in this inverse problem.

Table 1: The relative errors for μ_f using different λ ($\delta = 0.01$, $NL = 3$, $NN = 20$).

Error	$\lambda = 10000$	$\lambda = 1000$	$\lambda = 100$
Re_{μ_f}	$12.4927\% \pm 1.9310\%$	$7.9987\% \pm 0.5041\%$	$8.6146\% \pm 0.1949\%$
Error	$\lambda = 10$	$\lambda = 1$	$\lambda = 0.1$
Re_{μ_f}	$9.7343\% \pm 0.5150\%$	$16.1470\% \pm 1.5965\%$	$19.4545\% \pm 1.2732\%$

6 Conclusion and remark

In this work, the inverse dynamic source problem by the one single boundary measurement in finite time domain is considered, which is arising from the time-domain fluorescence diffuse optical tomography (FDOT). We establish the uniqueness theorem and the conditional stability of Lipschitz type for the inverse problem by a defined weighted norm. A deep neural network-based reconstruction scheme with a new loss function has been proposed to solve the inverse problem. Generalization error estimates based on the Lipschitz conditional stability of inverse problems have been established, which provide a measure of the stability and accuracy of the proposed method in solving the inverse problem. Some numerical experiments have been conducted, which indicate the effectiveness of the approach in this work.

Acknowledgments

Zhidong Zhang is supported by the National Key Research and Development Plan of China (Grant No. 2023YFB3002400), and National Natural Science Foundation of China (Grant No. 12101627). Chunlong Sun thanks National Natural Science Foundation of China (Grant Nos.12201298, 12274224), Natural Science Foundation of Jiangsu Province, China (Grant No. BK20210269) and "Double Innovation" Doctor of Jiangsu Province, China (Grant No.JSSCBS20220227). Mengmeng Zhang is supported by National Natural Science Foundation of China (Grant No.12301537), Natural Science Foundation of Hebei Province (Grant No.A2023202024) and Foundation of Tianjin Education Commission Research Program (Grant No.2022KJ102).

References

- [1] Shmuel Agmon, Avron Douglis, and Louis Nirenberg. Estimates near the boundary for solutions of elliptic partial differential equations satisfying general boundary conditions. i. *Communications on pure and applied mathematics*, 12:623–727, 1959. URL: <https://doi.org/10.1002/cpa.3160120405>, doi:10.1002/cpa.3160120405.
- [2] Simon R. Arridge. Optical tomography in medical imaging. *Inverse Problems*, 15(2):R41–R93, 1999. URL: <https://doi.org/10.1088/0266-5611/15/2/022>, doi:10.1088/0266-5611/15/2/022.
- [3] Simon R. Arridge and John C. Schotland. Optical tomography: forward and inverse problems. *Inverse Problems*, 25(12):123010, 59, 2009. URL: <https://doi.org/10.1088/0266-5611/25/12/123010>, doi:10.1088/0266-5611/25/12/123010.
- [4] Gang Bao, Xiaojing Ye, Yaohua Zang, and Haomin Zhou. Numerical solution of inverse problems by weak adversarial networks. *Inverse Problems*, 36(11):115003, 31, 2020. URL: <https://doi.org/10.1088/1361-6420/abb447>, doi:10.1088/1361-6420/abb447.
- [5] Johann Baumeister, Barbara Kaltenbacher, and Antonio Leitão. On Levenberg-Marquardt-Kaczmarz iterative methods for solving systems of nonlinear ill-

- posed equations. *Inverse Problems and Imaging*, 4(3):335–350, 2010. URL: <https://doi.org/10.3934/ipi.2010.4.335>, doi:10.3934/ipi.2010.4.335.
- [6] Yuyao Chen, Lu Lu, George Em Karniadakis, and Luca Dal Negro. Physics-informed neural networks for inverse problems in nano-optics and metamaterials. *Optics express*, 28(8):11618–11633, 2020. URL: <https://opg.optica.org/oe/abstract.cfm?URI=oe-28-8-11618>, doi:10.1364/OE.384875.
- [7] Teresa Correia, Maximilian Koch, Angelique Ale, Vasilis Ntziachristos, and Simon Arridge. Patch-based anisotropic diffusion scheme for fluorescence diffuse optical tomography - part 2: Image reconstruction. *Physics in Medicine and Biology*, 61(4):1452–1475, 2016.
- [8] Tim De Ryck, Ameya D Jagtap, and Siddhartha Mishra. Error estimates for physics-informed neural networks approximating the navier–stokes equations. *IMA Journal of Numerical Analysis*, 44(1):83–119, 2024. URL: <https://doi.org/10.1093/imanum/drac085>.
- [9] Chenguang Duan, Yuling Jiao, Yanming Lai, Dingwei Li, Xiliang Lu, and Jerry Zhijian Yang. Convergence rate analysis for deep Ritz method. *Communications in Computational Physics*, 31(4):1020–1048, 2022. URL: <https://doi.org/10.4208/cicp.oa-2021-0195>, doi:10.4208/cicp.oa-2021-0195.
- [10] Joyita Dutta, Sangtae Ahn, Changqing Li, Simon R Cherry, and Richard M Leahy. Joint l1 and total variation regularization for fluorescence molecular tomography. *Physics in Medicine and Biology*, 57(6):1459–1476, 2015.
- [11] Weinan E and Bing Yu. The deep Ritz method: a deep learning-based numerical algorithm for solving variational problems. *Communications in Mathematics and Statistics*, 6(1):1–12, 2018. URL: <https://doi.org/10.1007/s40304-018-0127-z>, doi:10.1007/s40304-018-0127-z.
- [12] Lawrence C. Evans. *Partial differential equations*, volume 19 of *Graduate Studies in Mathematics*. American Mathematical Society, Providence, RI, second edition, 2010. URL: <https://doi.org/10.1090/gsm/019>, doi:10.1090/gsm/019.
- [13] Martin Hanke. A regularizing levenberg - marquardt scheme, with applications to inverse groundwater filtration problems. *Inverse Problems*, 13(1):79–95, feb 1997. URL: <https://doi.org/10.1088/0266-5611/13/1/007>, doi:10.1088/0266-5611/13/1/007.
- [14] Martin Hanke, Andreas Neubauer, and Otmar Scherzer. A convergence analysis of the landweber iteration for nonlinear ill-posed problems. *Numerische Mathematik*, 72(1):21–37, 1995. doi:10.1007/s002110050158.
- [15] Qingguo Hong, Jonathan W. Siegel, and Jinchao Xu. Rademacher complexity and numerical quadrature analysis of stable neural networks with applications to numerical pdes. *arXiv preprint*. doi:arXiv:2104.02903.
- [16] Huabei Jiang. *Diffuse optical tomography: principles and applications*. CRC Press, Taylor & Francis Group, Boca Raton, 2011.

- [17] Yuling Jiao, Yanming Lai, Dingwei Li, Xiliang Lu, Fengru Wang, Yang Wang, and Jerry Zhijian Yang. A rate of convergence of physics informed neural networks for the linear second order elliptic PDEs. *Communications in Computational Physics*, 31(4):1272–1295, 2022. URL: <https://doi.org/10.4208/cicp.oa-2021-0186>, doi:10.4208/cicp.oa-2021-0186.
- [18] Qinian Jin and Min Zhong. On the iteratively regularized gauss-newton method in banach spaces with applications to parameter identification problems. *Numerische Mathematik*, 124(2013):647–683, 2013. doi:10.1007/s00211-013-0529-5.
- [19] Goro Nishimura Junyong Eom, Gen Nakamura and Chunlong Sun. Local analysis for locating a single point target in time-domain fluorescence diffuse optical tomography. *Differential and Integral Equations*, 37(1/2):27–58, 2024. URL: <https://doi.org/10.57262/die037-0102-27>, doi:10.57262/die037-0102-27.
- [20] B Kaltenbacher. A convergence rates result for an iteratively regularized gauss–newton–halley method in banach space. *Inverse Problems*, 31(1):015007, 2015. doi:10.1088/0266-5611/31/1/015007.
- [21] Kenneth Levenberg. A method for the solution of certain non-linear problems in least squares. *Quarterly of applied mathematics*, 2:164–168, 1944. URL: <https://doi.org/10.1090/qam/10666>, doi:10.1090/qam/10666.
- [22] Guang Lin, Zecheng Zhang, and Zhidong Zhang. Theoretical and numerical studies of inverse source problem for the linear parabolic equation with sparse boundary measurements. *Inverse Problems*, 38(12):Paper No. 125007, 28, 2022.
- [23] Jijun Liu, Manabu Machida, Gen Nakamura, Goro Nishimura, and Chunlong Sun. On fluorescence imaging: The diffusion equation model and recovery of the absorption coefficient of fluorophores. *Science China Mathematics*, 2020. doi:10.1007/s11425-020-1731-y.
- [24] Yan Liu, Wuwei Ren, and Habib Ammari. Robust reconstruction of fluorescence molecular tomography with an optimized illumination pattern. *Inverse Problems and Imaging*, 14(3):535–568, 2020. URL: <https://doi.org/10.3934/ipi.2020025>, doi:10.3934/ipi.2020025.
- [25] Lu Lu, Pengzhan Jin, Guofei Pang, Zhongqiang Zhang, and George Em Karniadakis. Learning nonlinear operators via deepnet based on the universal approximation theorem of operators. *Nature machine intelligence*, 3(3):218–229, 2021.
- [26] Lu Lu, Xuhui Meng, Zhiping Mao, and George Em Karniadakis. DeepXDE: a deep learning library for solving differential equations. *SIAM Review*, 63(1):208–228, 2021. URL: <https://doi.org/10.1137/19M1274067>, doi:10.1137/19M1274067.
- [27] Yulong Lu, Jianfeng Lu, and Min Wang. A priori generalization analysis of the deep ritz method for solving high dimensional elliptic partial differential equations. volume 134 of *Proceedings of Machine Learning Research*, pages 3196–3241. PMLR, 2021. URL: <https://proceedings.mlr.press/v134/lu21a.html>.
- [28] Tao Luo and Haizhao Yang. Two-layer neural networks for partial differential equations: Optimization and generalization theory, 2020. arXiv:2006.15733.

- [29] Donald W. Marquardt. An algorithm for least-squares estimation of nonlinear parameters. *Journal of the Society for Industrial and Applied Mathematics*, 11:431–441, 1963.
- [30] Fabrizio Martelli, Tiziano Binzoni, Samuele Del Bianco, André Liemert, and Alwin Kienle. *Light propagation through biological tissue and other diffusive media: theory, solutions, software*. SPIE Press, Bellingham, Washington, 2010.
- [31] Siddhartha Mishra and Roberto Molinaro. Estimates on the generalization error of physics-informed neural networks for approximating a class of inverse problems for PDEs. *IMA Journal of Numerical Analysis*, 42(2):981–1022, 2022. URL: <https://doi.org/10.1093/imanum/drab032>, doi:10.1093/imanum/drab032.
- [32] M. Raissi, P. Perdikaris, and G. E. Karniadakis. Physics-informed neural networks: a deep learning framework for solving forward and inverse problems involving nonlinear partial differential equations. *Journal of Computational Physics*, 378:686–707, 2019. URL: <https://doi.org/10.1016/j.jcp.2018.10.045>, doi:10.1016/j.jcp.2018.10.045.
- [33] Maziar Raissi, Alireza Yazdani, and George Em Karniadakis. Hidden fluid mechanics: A navier-stokes informed deep learning framework for assimilating flow visualization data, 2018. [arXiv:1808.04327](https://arxiv.org/abs/1808.04327).
- [34] William Rundell and Zhidong Zhang. On the identification of source term in the heat equation from sparse data. *SIAM Journal on Mathematical Analysis*, 52(2):1526–1548, 2020. URL: <https://doi.org/10.1137/19M1279915>, doi:10.1137/19M1279915.
- [35] Yeonjong Shin, Jérôme Darbon, and George Em Karniadakis. On the convergence of physics informed neural networks for linear second-order elliptic and parabolic type PDEs. *Communications in Computational Physics*, 28(5):2042–2074, 2020. URL: <https://doi.org/10.4208/cicp.oa-2020-0193>, doi:10.4208/cicp.oa-2020-0193.
- [36] Yeonjong Shin, Zhongqiang Zhang, and George Em Karniadakis. Error estimates of residual minimization using neural networks for linear pdes. *Journal of Machine Learning for Modeling and Computing*, 4(4):73–101, 2023. doi:10.1615/JMachLearnModelComput.2023050411.
- [37] Khemraj Shukla, Patricio Clark Di Leoni, James Blackshire, Daniel Sparkman, and George Em Karniadakis. Physics-informed neural network for ultrasound nondestructive quantification of surface breaking cracks. *Journal of Nondestructive Evaluation*, 39:1–20, 2020.
- [38] Justin Sirignano and Konstantinos Spiliopoulos. DGM: a deep learning algorithm for solving partial differential equations. *Journal of Computational Physics*, 375:1339–1364, 2018. URL: <https://doi.org/10.1016/j.jcp.2018.08.029>, doi:10.1016/j.jcp.2018.08.029.
- [39] Chunlong Sun and Jijun Liu. An inverse source problem for distributed order time-fractional diffusion equation. *Inverse Problems*, 36(5):055008, apr 2020. URL: <https://dx.doi.org/10.1088/1361-6420/ab762c>, doi:10.1088/1361-6420/ab762c.
- [40] Chunlong Sun and Jijun Liu. Reconstruction of the space-dependent source from partial neumann data for slow diffusion system. *Acta Mathematicae Applicatae Sinica, English*

- Series*, 36(1):166–182, 2020. URL: <https://doi.org/10.1007/s10255-020-0919-2>, doi:10.1007/s10255-020-0919-2.
- [41] Chunlong Sun and Zhidong Zhang. Uniqueness and numerical inversion in the time-domain fluorescence diffuse optical tomography. *Inverse Problems*, 38(10):104001, sep 2022. URL: <https://dx.doi.org/10.1088/1361-6420/ac88f3>, doi:10.1088/1361-6420/ac88f3.
- [42] Yaohua Zang, Gang Bao, Xiaojing Ye, and Haomin Zhou. Weak adversarial networks for high-dimensional partial differential equations. *Journal of Computational Physics*, 411:109409, 14, 2020. URL: <https://doi.org/10.1016/j.jcp.2020.109409>, doi:10.1016/j.jcp.2020.109409.
- [43] Mengmeng Zhang, Qianxiao Li, and Jijun Liu. On stability and regularization for data-driven solution of parabolic inverse source problems. *Journal of Computational Physics*, 474:111769, 2023. URL: <https://doi.org/10.1016/j.jcp.2022.111769>, doi:10.1016/j.jcp.2022.111769.